# Steady Deep-Water Waves On A Linear Shear Current

Thesis by
Jeffrey Alan Simmen

In Partial Fulfillment of the Requirements
for the Degree of
Doctor of Philosophy

California Institute of Technology
Pasadena, California
1984
(Submitted May 23, 1984)

ACKNOWLEDGEMENTS

I thank Caltech, the Office of Naval Research and the National Science Foundation (OCE-8100517) for supporting my research. I am also grateful to Dr. P.G. Saffman for being both a good friend and advisor.

For My Family

# ABSTRACT

The behavior of steady, periodic, deep-water gravity waves on a linear shear current is investigated. A weakly nonlinear approximation for the small amplitude waves is constructed via a variational principle. A local analysis of those large amplitude waves with sharp crests, called extreme waves, is also provided. To construct solutions for all waveheights (especially the limiting ones) a convenient mathematical formulation which involves only the wave profile and some constants of the motion is derived and then solved by numerical means. It is found that for some shear currents the highest waves are not necessarily the extreme waves. Furthermore a certain non-uniqueness in the sense of a fold is shown to exist and a new type of limiting wave is discovered.

TABLE OF CONTENTS

# LIST OF FIGURES

# INTRODUCTION

Water waves are a fascinating element of nature and the study of them is motivated for both aesthetic and practical reasons. From a practical viewpoint a better understanding of water waves is essential in improving the design of coastal and offshore structures. It would also be beneficial to the engineering of devices that harness water wave energy.

Since the 1800s a sizeable effort has gone into the study of gravity waves on the surface of deep water. Its major emphasis has been on steady, one-dimensional, periodic waves where usually the water has been assumed inviscid and its motion irrotational. Realistically, the second assumption is often invalid and the study of waves on shear currents is perhaps better.

The classic irrotational work was done by Stokes (1847). Using a perturbation series in essentially wave amplitude he constructed a weakly nonlinear approximation to nonlinear waves. He also conjectured that the highest wave should have a corner at the crest with an included angle of $120^{o}$. Over a century later Amick, Fraenkel & Toland (1982) rigorously confirmed the existence of such a singular wave from the equations but were unable to verify that this so-called extreme wave was also the wave of greatest height. By forcing this singular nature into a form of the solution Michell (1893), Yamada (1957) and Rottman & Olfe (1980) were all able to calculate approximate extreme waves. The behavior of almost-extreme waves was explored by Longuet-Higgins & Fox (1978). They matched an inner solution valid near the crest with an outer solution valid in the rest of the wave and discovered that the energies and wavespeed are oscillatory functions of waveheight. From numerical computations, Chen & Saffman (1980) discovered new branches of solutions that they called irregular

waves and McLean (1982) investigated the stability of irrotational deep-water waves to infinitesimal three-dimensional perturbations.

Some attempts in understanding the more difficult problem of finite-amplitude rotational water waves have also been made. Gerstner (1802) found the earliest finite amplitude solution but it had a vorticity distribution that was singular at the free surface of the highest wave. For finite depth Tsao (1959) developed an algebraically complicated Stokes-type approximation for waves on a linear shear current (uniform vorticity). For these same waves Dalrymple (1974) numerically approximated solutions by using a truncated Fourier series representation for the stream function. His method would be incapable of high wave calculations though. Later Dalrymple (1976,1977) numerically investigated finite amplitude waves on other current profiles. For rotational flows in general Miche (1944) argued that the highest wave should have a $120^{\circ}$ corner at the crest.

The focus of this study is deep-water waves on a linear shear current, and a special effort is made to investigate the properties of large amplitude waves up to and including the limiting waves. In chapter 1 the physical problem is clearly stated and a useful mathematical description of it is rigorously derived. Also in this chapter some integral properties of the waves are formulated. In chapter 2 a weakly nonlinear approximation by way of a variational principle is constructed. The nature of the extreme waves is investigated in chapter 3. Chapter 4 gives a description of the numerical method used to connect the weakly nonlinear waves of the second chapter to the extreme waves of the third chapter, and chapter 5 is a discussion of the results. A brief note on stability is included in chapter 6.

# CHAPTER 1

# MATHEMATICAL FORMULATION

This study concerns one-dimensional, periodic, symmetric water waves of permanent form, propagating through an otherwise vertically varying shear current. It is restricted to the case of deep water in a constant gravitational field, where both the surface tension of the water and the density of the upper fluid (air) are neglected. The theory is inviscid, and so the shear is assumed to have been produced by external effects.

## 1.1. **Water waves on a deep linear shear current**

We first describe the undisturbed flow: a shear current that varies linearly in the vertical direction. Choose rectangular coordinates $(x', y')$ with the $x'$ -axis horizontal and the $y'$ -axis vertical, so that the undisturbed water surface is given by $y' = 0$. Then the horizontal velocity, $u'$, and the vertical velocity, $v'$, of the current are given by

$$u' = \Omega y' + d$$
$$v' = 0$$

where $\Omega$ specifies the magnitude of the shear. The water surface has $y' = 0$ and consequently the pressure in the water, $p'$, will satisfy

$$p' = p_0 - gy'$$

where $p_0$ is the constant air pressure, $g$ is the gravitational acceleration constant, and without loss of generality the density of the water is taken equal to 1. By choosing axes which move with the necessary horizontal velocity we can make $u'$ vanish at the surface, and so we may take $d = 0$. The water depth is taken to be infinite, and then initially the picture in figure 1-1 holds.

Our interest is in wave propagation on this shear flow. If $p'$ is the pressure and $\vec{u}' = (u', v')$ is the velocity vector in the $(x', y')$ coordinate system, the two-dimensional equations of motion for an incompressible, inviscid fluid with density equal to 1 are

$$\nabla' \cdot \vec{u}' = 0 \tag{1.1.1}$$

$$\frac{\partial \vec{u}'}{\partial t} + [\vec{u}' \cdot \nabla']\vec{u}' = -\nabla' p' - (0, g) \quad ; \tag{1.1.2}$$

where $\nabla' = (\frac{\partial}{\partial x'}, \frac{\partial}{\partial y'})$ and the notation $(a, b)$ is used to represent a vector with horizontal component $a$ and vertical component $b$.

Define $\omega$, a measure of the vorticity, by $\omega = \frac{\partial u'}{\partial y'} - \frac{\partial v'}{\partial x'}$. And define the two-dimensional vector operator, $curl'$, by $curl'(a, b) = \frac{\partial b}{\partial x'} - \frac{\partial a}{\partial y'}$. Then if the $curl'$ of equation (1.1.2) is taken we obtain

$$\frac{\partial \omega}{\partial t} + [\vec{u}' \cdot \nabla']\omega = 0 \qquad \text{(vorticity equation)} \quad . \tag{1.1.3}$$

Equation (1.1.3) simply states that $\omega$ is a constant following a fluid particle. Thus, if initially $\omega = \Omega$ everywhere in the fluid (as in the case for our original shear flow), then $\omega = \Omega$ for all time. This is the key point that makes this constant vorticity problem so much more approachable than the general vorticity case.

Because $curl'\, \vec{u}' = -\Omega$ always, $curl'\, [\vec{u}' - (\Omega y', 0)] = 0$ always. Hence a potential $\varphi'$ exists where

$$\vec{u}' = \nabla' \varphi' + (\Omega y', 0) \quad . \tag{1.1.4}$$

Of course $\varphi'$ is arbitrary to within a function of $t$; however, it can be uniquely specified and at the same time made to satisfy the "bottom" boundary condition of

$$\vec{u}' \to (\Omega y', 0) \quad \text{(uniformly in } x') \quad \text{as} \quad y' \to -\infty \tag{1.1.5}$$

by requiring that

$$\varphi' \to 0 \quad \text{(uniformly in } x') \quad \text{as} \quad y' \to -\infty \quad . \tag{1.1.6}$$

Substitution of equation (1.1.4) into equation (1.1.1) gives

$$\nabla'^2 \varphi' = 0 \quad , \tag{1.1.7}$$

which means that $\varphi'$ is harmonic. Since the fluid domain is simply connected, $\psi'$ (its harmonic conjugate) exists and is defined by

$$\frac{\partial \psi'}{\partial x'} = -\frac{\partial \varphi'}{\partial y'}$$

$$\frac{\partial \psi'}{\partial y'} = \frac{\partial \varphi'}{\partial x'} \quad .$$

As before, we uniquely fix $\psi'$ so that $\psi' \to 0$ (uniformly in $x'$) as $y' \to -\infty$. The expression of the velocity in terms of $\psi'$ is clearly just

$$\vec{u}' = \left(\frac{\partial \psi'}{\partial y'} + \Omega y', -\frac{\partial \psi'}{\partial x'}\right) \quad . \tag{1.1.8}$$

At this point we derive a "Bernoulli-type" equation. Consider the vector identity,

$$[\vec{u}' \cdot \nabla']\vec{u}' = \nabla'\left[\tfrac{1}{2}\vec{u}' \cdot \vec{u}'\right] + \omega(v', -u') \quad ;$$

where $\omega = \frac{\partial u'}{\partial y'} - \frac{\partial v'}{\partial x'}$. This identity when $\omega = \Omega$, along with relations (1.1.4) and (1.1.8), allow us to rewrite equation (1.1.2) as

$$\nabla'\left(\frac{\partial \varphi'}{\partial t} + \tfrac{1}{2}\left[\frac{\partial \varphi'}{\partial x'} + \Omega y'\right]^2 + \tfrac{1}{2}\left[\frac{\partial \varphi'}{\partial y'}\right]^2 - \Omega \psi' - \tfrac{1}{2}\Omega^2 y'^2\right) = -\nabla'\left(p' + g y'\right) \quad .$$

This may be integrated to

$$\frac{\partial \varphi'}{\partial t} + \tfrac{1}{2}\left[\frac{\partial \varphi'}{\partial x'}\right]^2 + \tfrac{1}{2}\left[\frac{\partial \varphi'}{\partial y'}\right]^2 + \Omega y' \frac{\partial \varphi'}{\partial x'} - \Omega \psi' + g y' = -[p' - p_0] + F(t)$$

where $p_0$ is the air pressure separated from the arbitrary function $F(t)$. Since by choice $\varphi'$ , $\psi' \to 0$ as $y' \to -\infty$, taking the limit as $y' \to -\infty$ of this last equation we find that $F(t) \equiv 0$. Here the pressure behavior at large depth which is

$$p' - p_0 + gy' \to 0 \quad \text{as} \quad y' \to -\infty$$

has been used.

Therefore, we have derived

$$\frac{\partial \varphi'}{\partial t} + \frac{1}{2}\left[\frac{\partial \varphi'}{\partial x'}\right]^2 + \frac{1}{2}\left[\frac{\partial \varphi'}{\partial y'}\right]^2 + \Omega y' \frac{\partial \varphi'}{\partial x'} - \Omega \psi' + gy' = -[p' - p_0] \quad . \quad (1.1.9)$$

Next boundary conditions are detailed. Since the forces on the two sides of the air and water interface must be equal, ignoring surface tension we must have that $p' = p_0$ at $y' = \eta'(x', t)$; where $y' = \eta'(x', t)$ describes the interface, and $p_0$ is the undisturbed air pressure. (Pressure changes in the air due to its motion are negligible.) Applying this to equation (1.1.9) gives

$$\frac{\partial \varphi'}{\partial t} + \frac{1}{2}\left[\frac{\partial \varphi'}{\partial x'}\right]^2 + \frac{1}{2}\left[\frac{\partial \varphi'}{\partial y'}\right]^2 + \Omega y' \frac{\partial \varphi'}{\partial x'} - \Omega \psi' + gy' = 0 \quad \text{on} \quad y' = \eta'(x', t) \quad . \quad (1.1.10)$$

This is the dynamic condition at the surface.

The kinematic condition comes from the usual argument that particles in the surface remain there or

$$\left[\frac{\partial}{\partial t} + \vec{u}'(x', \eta') \cdot \nabla'\right] [y' - \eta'(x', t)] = 0 \quad .$$

After replacement of the velocity by terms involving the potential, this may be rewritten as

$$\frac{\partial \eta'}{\partial t} + \left[\frac{\partial \varphi'}{\partial x'} + \Omega y'\right] \frac{\partial \eta'}{\partial x'} = \frac{\partial \varphi'}{\partial y'} \quad \text{on} \quad y' = \eta'(x', t) \quad . \quad (1.1.11)$$

### 1.2. Waves of permanent form

Our interest is in waves of permanent form, also known as steady waves. By definition then, there will exist a frame of reference moving with constant velocity $(c, 0)$ relative to the $(x', y')$ coordinate system, within which the motion will be viewed as steady. If the coordinates in this new frame are $(x, y)$ and the velocity in it is $\vec{u} = (u, v)$ then we have the transformation:

$$x = x' - ct$$
$$y = y'$$
$$u(x,y) = u'(x',y',t) - c$$
$$v(x,y) = v'(x',y',t) \quad .$$

The quantity $c$ is by our definition the phase velocity, and is sometimes referred to as the wave speed.

An implication of the steady motion is that there exist functions $\varphi$, $\psi$ and $H$ dependent on the position $(x,y)$ only and such that

$$\varphi(x,y) = \varphi'(x',y',t)$$
$$\psi(x,y) = \psi'(x',y',t)$$
$$H(x) = \eta'(x',t) \quad .$$

It follows that

$$\vec{u} = \nabla\varphi + (\Omega y - c, 0) \tag{1.2.1}$$

and

$$\vec{u} = \left(\frac{\partial\psi}{\partial y} + \Omega y - c, -\frac{\partial\psi}{\partial x}\right) \tag{1.2.2}$$

where $\nabla = \left(\frac{\partial}{\partial x}, \frac{\partial}{\partial y}\right)$. Since in this steady frame derivatives with respect to the time variable $t$ are zero it also follows that the kinematic condition (1.1.11) is equivalent to

$$\frac{d}{dx}[\psi(x,H) + \tfrac{1}{2}\Omega H^2 - cH] = 0 \quad .$$

After integration this becomes

$$\psi(x,y) + \tfrac{1}{2}\Omega y^2 - cy = \psi_0 \quad \text{on} \quad y = H(x) \quad . \tag{1.2.3}$$

This discovery is just the statement that $\psi + \frac{1}{2}\Omega y^2 - cy$ is the usual stream-function which is equal to a constant $\psi_0$ on the free surface.

At last we put together for our permanent form waves the nonlinear system of equations that must be satisfied by the potential $\varphi(x,y)$ and the profile $H(x)$. From (1.1.7) the equation for $\varphi$ which must hold in the entire fluid

domain is Laplace's equation:

$$\nabla^2\varphi = 0 \quad \text{in} \quad -\infty < y < H(x) \quad . \tag{1.2.4a}$$

After eliminating $\psi$ in (1.1.10) by using (1.2.3), the dynamic condition which must hold at the surface is

$$\tfrac{1}{2}\left[\frac{\partial\varphi}{\partial x} + \Omega y - c\right]^2 + \tfrac{1}{2}\left[\frac{\partial\varphi}{\partial y}\right]^2 + gy = B \quad \text{on} \quad y = H(x) \quad , \tag{1.2.4b}$$

where $B = \Omega\psi_0 + \frac{1}{2}c^2$ is a constant. From (1.1.11) the kinematic condition at the surface is

$$\left[\frac{\partial\varphi}{\partial x} + \Omega y - c\right]\frac{dH}{dx} = \frac{\partial\varphi}{\partial y} \quad \text{on} \quad y = H(x) \quad . \tag{1.2.4c}$$

We also need to add the condition at the bottom which from (1.1.6) is

$$\varphi \to 0 \quad (\text{uniformly in } x) \quad \text{as} \quad y \to -\infty \quad . \tag{1.2.4d}$$

These are the time independent equations for steady waves in the $(x\,,y)$ coordinate system. Note that periodicity and symmetry have not yet been imposed.

A simple observation reveals that if $c$, $\varphi(x,y)$, $H(x)$ and $B$ are solutions to (1.2.4) for $\Omega$, then $-c$, $-\varphi(x,y)$, $H(x)$ and $B$ are solutions for $-\Omega$. This means that there is no loss of generality if the study is restricted to waves with positive speeds $(c > 0)$ so long as both positive and negative shears (all $\Omega$) are considered.

### 1.3. Periodic and symmetric waves

By working in the complex plane we reduce the calculation of the profile of a steady, periodic and symmetric wave to the solution of a nonlinear integro-differential equation.

Presently it is worth noting that if $H(x)$ and $\varphi(x\,,y)$ are solutions to equations (1.2.4) then so are $H(-x)$ and $-\varphi(-x\,,y)$ for the same $c$, $B$, and $\Omega$. This is a necessary condition for symmetric waves to exist, and so the assumption of

symmetry is consistent with the equations.

Let $x$ and $y$ be the coordinates as before (in the steady frame) and introduce the complex variable

$$z = x + iy \quad .$$

Then the complex function

$$w(z) = \varphi(x, y) + i\psi(x, y)$$

is an analytic function of $z$ in the fluid domain of the $z$-plane. This holds by equation (1.2.4a) and the definition of $\psi$ as the harmonic conjugate of $\varphi$. $\Delta(z)$, where

$$\Delta(z) = \frac{dw}{dz} \left( \equiv \frac{\partial \varphi}{\partial x} - i \frac{\partial \varphi}{\partial y} \right) \quad ,$$

will be analytic in the same domain. If the curve $y = H(x)$ is parametrized by

$$\begin{aligned} x &= \alpha(\tau) \\ y &= \beta(\tau) \quad , \quad -\infty < \tau < \infty \quad , \end{aligned}$$

then in the complex plane $z = \alpha(\tau) + i\beta(\tau)$ will describe the wave profile. This allows us to calculate profiles which cannot be described by $y = H(x)$, where $H(x)$ is a single-valued function of $x$. Although at this point the parameter $\tau$ is not specified, we remove some arbitrariness by fixing the origin and direction of the $\tau$ parameter so that

$$\alpha(0) = 0 \tag{1.3.1a}$$

and

$$\left. \frac{d\alpha}{d\tau} \right|_{\tau=0} \geq 0 \quad , \tag{1.3.1b}$$

respectively. For convenience let

$$\zeta(\tau) \equiv \alpha(\tau) + i\beta(\tau) \quad .$$

Our interest is in periodic waves. Given the wavelength $\lambda$, these waves satisfy $\Delta(z + \lambda) = \Delta(z)$. Furthermore there will exist a length called $d$ which is

dependent on the parameter $\tau$, such that $\zeta(\tau+d) = \zeta(\tau) + \lambda$. As in Chen & Saffman (1980) we will study the wave in a window of horizontal extent $\Lambda$, where $\Lambda$ is an integral multiple of the wavelength; that is, $\Lambda = n\lambda$, $n$ a positive integer. Likewise, if $D$ is defined by $D = nd$ then it follows that $\zeta(\tau+D) = \zeta(\tau) + \Lambda$. Consequently we need only study $\zeta(\tau)$ for $0 \leq \tau < D$.

We want to restrict our attention to symmetric waves. Let us force symmetry about $\tau = \frac{1}{2}D$ by requiring that

$$\zeta(\tau) = \Lambda - \overline{\zeta}(D-\tau) \quad , \quad 0 \leq \tau < D \quad . \tag{1.3.2}$$

Then by periodicity $\tau = 0$ and $\tau = D$ must both be crests or troughs of the wave profile. Since $\tau = 0$ corresponds to $x = 0$, this symmetry locates the origin of the $x$-coordinate at either a crest or trough. (Later the origin is specifically placed at a crest.)

Recall that the origin of the $y$-coordinate was fixed when we located the initial (undisturbed) water surface at $y = 0$. Because of the fluid incompressibility this means that the wave surface will always have a mean height equal to zero or mathematically,

$$\int_0^D \beta(\tau)\frac{d\alpha}{d\tau}d\tau = 0 \quad . \tag{1.3.3}$$

We are now in a position to begin the derivation of the integro-differential equation. Application of the Cauchy integral formula gives the relation

$$\Delta(z) = \frac{1}{2\pi i}\int_\Gamma \frac{\Delta(\hat{z})}{z-\hat{z}}d\hat{z} \quad ,$$

where $\Gamma$ is any closed contour in the fluid domain of the $\hat{z}$-plane which encloses $z$ in a clockwise manner. Pick $\Gamma$ so that with $m$ a positive integer, $\Gamma = \Gamma_1(m) + \Gamma_2(m)$ is the dotted contour in figure 1-2. $\Gamma_1(m)$ consists of a section of the wave profile containing $2m$ cycles and is described by $\hat{z} = \zeta(\hat{\tau}) \equiv \alpha(\hat{\tau}) + i\beta(\hat{\tau})$, $-mD < \hat{\tau} < mD$. $\Gamma_2(m)$ is a semi-circular arc of

radius $m\Lambda$ and centered at $\zeta(0)$. We should mention that for the special case of the extreme wave (which is discussed later) $\Delta(\hat{z})$ is apparently not analytic at a $120^\circ$ corner point of $\Gamma_1$; however, the Cauchy Integral Formula still holds as $\Delta(\hat{z})$ is continuous onto $\Gamma_1$ at that point. Separating the contour into two parts means that if

$$R_m(z) = \frac{1}{2\pi i}\int_{\Gamma_2(m)} \frac{\Delta(\hat{z})}{z-\hat{z}}\,d\hat{z} \tag{1.3.4}$$

then obviously

$$\Delta(z) = \frac{1}{2\pi i}\int_{\Gamma_1(m)} \frac{\Delta(\hat{z})}{z-\hat{z}}\,d\hat{z} + R_m(z) \quad .$$

In the limit as $z \to \zeta(\tau)$, $0 \le \tau < D$, we use Plemelj's formula to deduce that

$$\Delta(\tau) = \frac{1}{2\pi i}\,\text{⨍}_{-mD}^{mD} \frac{\Delta(\hat{\tau})}{\zeta(\tau)-\zeta(\hat{\tau})}\frac{d\zeta}{d\hat{\tau}}\,d\hat{\tau} + \frac{\kappa(\tau)}{2}\Delta(\tau) + R_m(\zeta(\tau)) \quad , \tag{1.3.5}$$

where $\Delta(\tau)$ denotes $\Delta(\zeta(\tau))$ and ⨍ denotes the Cauchy principal value integral. With the exception of the extreme wave which has a slope discontinuity at the crest

$$\kappa(\tau) \equiv 1 \quad , \quad \text{for all } \tau \quad .$$

For the extreme wave which has a $120^\circ$ corner at the crest

$$\kappa(\tau) = \begin{cases} \frac{4}{3} & \text{if } \tau \text{ is the position of a } 120^\circ \text{ corner} \\ 1 & \text{otherwise} \end{cases} .$$

(See Muskhelishvili, 1946.)

Let us investigate the behavior of $R_m(z)$ for large $m$. Integrate (1.3.4) once by parts and use $\Delta(z) = \frac{dw}{dz}$ to obtain

$$R_m(z) = \frac{1}{2\pi i}\frac{w(\hat{z})}{z-\hat{z}}\bigg|_{\Gamma_2(m)} - \frac{1}{2\pi i}\int_{\Gamma_2(m)} \frac{w(\hat{z})}{(z-\hat{z})^2}\,d\hat{z} \quad .$$

In Appendix 1 a simple argument utilizing condition (1.2.4d) shows that $|w(\hat{z})|$ is bounded for all $\hat{z}$ in the region consisting of the fluid domain and its

boundary. It is also clear that $|\hat{z}-z| = O(m\Lambda)$ as $m \to \infty$ for $\hat{z} \in \Gamma_2(m)$. Since the length of $\Gamma_2(m)$ is equal to $\pi m\Lambda$ it follows that

$$|R_m(z)| = O(\frac{1}{2\pi m\Lambda}) + O(\frac{\pi m\Lambda}{2\pi m^2\Lambda^2}) \quad \text{as} \quad m \to \infty$$

and hence

$$R_m(z) \to 0 \quad \text{as} \quad m \to \infty \quad . \tag{1.3.6}$$

The implications of periodicity are found in Appendix 2 where it is proven that if $f(\tau)$ is some function satisfying $f(\tau+mD) = f(\tau)$, then

$$\int_{-mD}^{mD} \frac{f(\hat{\tau})}{\zeta(\tau)-\zeta(\hat{\tau})}\, d\hat{\tau} \;\to\; \frac{\pi}{\Lambda}\int_0^D f(\hat{\tau})\, \cot\left(\frac{\pi}{\Lambda}[\zeta(\tau)-\zeta(\hat{\tau})]\right) d\hat{\tau} \quad \text{as} \quad m \to \infty \quad . \tag{1.3.7}$$

A related formula verified in Appendix 3 is

$$\frac{-i}{\Lambda}\int_0^D \cot\left(\frac{\pi}{\Lambda}[\zeta(\tau)-\zeta(\hat{\tau})]\right) \frac{d\zeta}{d\hat{\tau}}\, d\hat{\tau} = 1-\kappa(\tau) \quad . \tag{1.3.8}$$

If we now utilize (1.3.6) and (1.3.7) in the limit as $m \to \infty$ of equation (1.3.5) and then use (1.3.8) to subtract off the singularity, we can derive that

$$\Delta(\tau) = -\frac{i}{\Lambda}\int_0^D [\Delta(\hat{\tau})-\Delta(\tau)]\, \cot\left(\frac{\pi}{\Lambda}[\zeta(\tau)-\zeta(\hat{\tau})]\right) \frac{d\zeta}{d\hat{\tau}}\, d\hat{\tau} \quad . \tag{1.3.9}$$

It is important to note that the principal value integral and the function $\kappa(\tau)$ do not appear in this formula. This means that (1.3.9) is nonsingular and its form is independent of whether it describes an extreme wave or a smooth wave.

Next form the functions $N(\tau)$, $q(\tau)$ and $n(\tau)$ using

$$N(\tau) = + \left(\frac{d\zeta}{d\tau}\,\frac{d\overline{\zeta}}{d\tau}\right)^{\frac{1}{2}}$$

and

$$q - in = \frac{1}{N(\tau)}\,\frac{d\zeta}{d\tau}\,[\Delta(\tau) + \Omega\beta(\tau) - c] \quad .$$

$N(\tau)$ determines the parametrization and will be discussed later. It can be shown that in the steady frame $q(\tau)$ is the tangential component and $n(\tau)$ is

the normal component of the fluid velocity at the wave surface. Easily computed is

$$\Delta(\tau) = \frac{1}{N(\tau)} \frac{d\overline{\zeta}}{d\tau} \left( q - in - \frac{[\Omega\beta - c]}{N} \frac{d\zeta}{d\tau} \right) \quad . \tag{1.3.10}$$

After some algebra, equations (1.2.4c) and (1.2.4b) can be shown equivalent to

$$n(\tau) = 0 \tag{1.3.11}$$

and

$$q^2(\tau) = 2B - 2g\beta(\tau) \quad . \tag{1.3.12}$$

Obviously, (1.3.11) is a statement that the free surface is a streamline. Equations (1.3.10) and (1.3.11) can be used in (1.3.9) to eliminate $\Delta(\tau)$ and $n(\tau)$ yielding

$$\frac{q(\tau)}{N(\tau)} \frac{d\overline{\zeta}}{d\tau} - \Omega\beta(\tau) + c = -\frac{i}{\Lambda} \int_0^D \left\{ q(\hat{\tau}) N(\hat{\tau}) - \frac{q(\tau)}{N(\tau)} \frac{d\overline{\zeta}}{d\tau} \frac{d\zeta}{d\hat{\tau}} + \right.$$

$$\left. \Omega[\beta(\tau) - \beta(\hat{\tau})] \frac{d\zeta}{d\hat{\tau}} \right\} \cot\left( \frac{\pi}{\Lambda} [\zeta(\tau) - \zeta(\hat{\tau})] \right) d\hat{\tau} \quad . \tag{1.3.13}$$

If (1.3.12) is thought of as the equation for $q(\tau)$, then (1.3.13) should be interpreted as the principal equation for the profile $\zeta(\tau)$.

### 1.4. Parametrization and complete formulation

In our formulation we have not yet specified the parameter $\tau$ but now shall do so. If $s$ is the arclength parameter such that $\frac{ds}{d\tau} \geq 0$ then it is known that

$$\frac{ds}{d\tau} = N(\tau)$$

since from a previous definition,

$$N(\tau) = + \left( \left[ \frac{d\alpha}{d\tau} \right]^2 + \left[ \frac{d\beta}{d\tau} \right]^2 \right)^{\frac{1}{2}} \quad .$$

The obvious conclusion is that the function $N(\tau)$ determines the parametrization.

Since we are free to choose $N(\tau)$ we make the selection

$$N(\tau) = -L\, q(\tau) \quad , \tag{1.4.1}$$

where $L$ is picked so that $D = 2\pi$. In Appendix 4 it is proven that $L$ must satisfy

$$L \int_0^{2\pi} q^2(\tau)\, d\tau = c\Lambda \quad . \tag{1.4.2}$$

We remark ahead of time that $N(\tau) > 0$ except for the case of the extreme wave where $N(0) = 0$. Since $\frac{ds}{d\tau} = N(\tau)$, this means that $\left.\frac{ds}{d\tau}\right|_{\tau=0} \to 0$ in the limit of the extreme wave. Therefore, in this limit a mesh with constant width in $\tau$ will concentrate more and more points at the crest. This is exactly what is desired for near extreme waves where the curvature changes very rapidly at the crest.

Finally we are ready to completely formulate our problem. Use (1.4.1) and (1.3.12) in (1.3.13) to eliminate $q(\tau)$ and $N(\tau)$ and thereby obtain

$$\frac{d\overline{\zeta}}{d\tau} + \Omega L \operatorname{Im}\zeta(\tau) - cL = -\frac{i}{\Lambda}\int_0^{2\pi} \Big\{ L^2[2B - 2g \operatorname{Im}\zeta(\hat{\tau})] -$$

$$\Omega L[\operatorname{Im}\zeta(\tau) - \operatorname{Im}\zeta(\hat{\tau})]\, \frac{d\zeta}{d\hat{\tau}} - \frac{d\overline{\zeta}}{d\tau}\frac{d\zeta}{d\hat{\tau}} \Big\}\, \cot\Big(\frac{\pi}{\Lambda}[\zeta(\tau) - \zeta(\hat{\tau})]\Big)\, d\hat{\tau} \tag{1.4.3a}$$

for $0 \le \tau < 2\pi$. $\operatorname{Im}\zeta(\tau)$ and $2\pi$ have been substituted for $\beta(\tau)$ and $D$, respectively. Combine (1.3.12) and (1.4.2) to yield

$$L \int_0^{2\pi} [2B - 2g \operatorname{Im}\zeta(\tau)]\, d\tau = c\Lambda \quad . \tag{1.4.3b}$$

To uniquely formulate the problem (1.4.3a) and (1.4.3b) need to be supplemented with the relations (1.3.1)-(1.3.3) which in that order are now

$$\operatorname{Re}\zeta(0) = 0 \tag{1.4.3c}$$

$$\zeta(\tau) = \Lambda - \overline{\zeta}(2\pi - \tau) \tag{1.4.3d}$$

and

$$\int_0^{2\pi} [\operatorname{Im}\zeta(\tau)]\, [\operatorname{Re}\frac{d\zeta}{d\tau}]\, d\tau = 0 \quad . \tag{1.4.3e}$$

Lastly add a condition that specifies the magnitude of the wave. It is sufficient

to give the waveheight, $h$, by

$$h = \max_{0\le\tau<2\pi}[\mathrm{Im}\,\zeta(\tau)] - \min_{0\le\tau<2\pi}[\mathrm{Im}\,\zeta(\tau)] \quad . \tag{1.4.3f}$$

It is this system of equations (1.4.3) that will be discretized and will allow us to numerically compute approximate wave profiles and wave speeds - even for extreme and almost-extreme waves, which are not resolved by other methods or formulations.

### 1.5. Integral properties

One integral property we wish to calculate is the excess kinetic energy per wavelength due to the presence of the wave. This quantity is measured in the original unsteady frame. Recall from section 1.2 that $(u', v') = (u+c, v)$ where $(u', v')$ and $(u, v)$ are the velocity in the unsteady and steady frame, respectively. Then it is clear that the average excess kinetic energy may be defined by

$$T = \frac{1}{\lambda}\int_0^\lambda \int_{-\infty}^{H(x)} \frac{1}{2}[(u+c)^2+v^2]\,dy\,dx - \frac{1}{\lambda}\int_0^\lambda \int_{-\infty}^{0} \frac{1}{2}\Omega^2 y^2\,dy\,dx \quad . \tag{1.5.1}$$

Also of interest are the mean potential energy defined by

$$P = \frac{1}{\lambda}\int_0^\lambda \int_0^{H(x)} gy\,dy\,dx \tag{1.5.2}$$

and the excess impulse per wavelength given by

$$I = \frac{1}{\lambda}\int_0^\lambda \int_{-\infty}^{H(x)} (u+c)\,dy\,dx - \frac{1}{\lambda}\int_0^\lambda \int_{-\infty}^{0} \Omega y\,dy\,dx \quad . \tag{1.5.3}$$

As before, we wish to rewrite our formulas for these integral properties in terms of our parameter $\tau$ so that they will hold even if the wave profile is not a single-valued function of $x$. At the same time considerable simplification can be made if we introduce the functions $\varphi$ and $\psi$ and use Stokes' Theorem. For example, with some manipulation we can show that (1.5.1) is equivalent to

$$2\lambda T = \int_0^\lambda \int_{-\infty}^{H(x)} curl\left(-\psi\frac{\partial\varphi}{\partial x}, -\psi\frac{\partial\varphi}{\partial y} + 2\Omega y\varphi\right) dy\,dx \;+$$

$$\int_0^{\lambda} \int_0^{H(x)} curl\left(-\tfrac{1}{3}\Omega^2 y^3, 0\right) dy\, dx \quad .$$

The operator $curl$ has been defined by $curl(a, b) = \dfrac{\partial b}{\partial x} - \dfrac{\partial a}{\partial y}$. Using the decay of $\varphi$ and $\psi$ as $y \to -\infty$, periodicity, Stokes' Theorem, and the parametric form for the wave profile this reduces to

$$2\lambda T = \int_0^d \psi(\alpha,\beta) \frac{d\varphi}{d\tau} d\tau - 2\Omega \int_0^d \beta(\tau)\, \varphi(\alpha,\beta) \frac{d\beta}{d\tau} d\tau + \tfrac{1}{3}\Omega^2 \int_0^d \beta^3(\tau) \frac{d\alpha}{d\tau} d\tau \quad .$$

Here $\dfrac{d\varphi}{d\tau}$ has been used to denote the derivative of $\varphi$ along $(\alpha(\tau), \beta(\tau))$, i.e.

$$\frac{d\varphi}{d\tau} = \frac{\partial \varphi}{\partial x} \frac{d\alpha}{d\tau} + \frac{\partial \varphi}{\partial y} \frac{d\beta}{d\tau} \quad .$$

By using (1.2.3), periodicity, and integration by parts we can finally show that

$$2\lambda T = \int_0^d \left[c\beta + \tfrac{1}{2}\Omega\beta^2\right] \frac{d\varphi}{d\tau} d\tau + \tfrac{1}{3}\Omega^2 \int_0^d \beta^3 \frac{d\alpha}{d\tau} d\tau \quad . \qquad (1.5.4)$$

In a similar manner we can deduce that

$$\lambda I = \int_0^d \beta \frac{d\varphi}{d\tau} d\tau + \tfrac{1}{2}\Omega \int_0^d \beta^2 \frac{d\alpha}{d\tau} d\tau \quad , \qquad (1.5.5)$$

while a simple application of Stokes' Theorem reveals that

$$\lambda P = \tfrac{1}{2} g \int_0^d \beta^2 \frac{d\alpha}{d\tau} d\tau \quad . \qquad (1.5.6)$$

For the case of $\Omega = 0$ our kinetic energy formula becomes $2\lambda T = c \int \beta\, d\varphi$. The relation $2T = cI$ also holds. These check with the results of Longuet-Higgins (1975) for irrotational waves.

In order that these integral properties may be directly calculated from only the wave profile and the various constants of the motion we need only make the substitution

$$\frac{d\varphi}{d\tau} = -\left[Lq^2 + (\Omega\beta - c) \frac{d\alpha}{d\tau}\right]$$

with

$$q^2 = 2(B - g\beta(\tau))$$

into the integrals of (1.5.4) and (1.5.5).

If in (1.5.3) equations (1.2.3) and $u - (\Omega y - c) = \frac{\partial \psi}{\partial y}$ are used, then since the mean wave height is zero the relation $I = \psi_0$ can be obtained. This may be used as a check for the numerical computations when $\Omega \neq 0$.

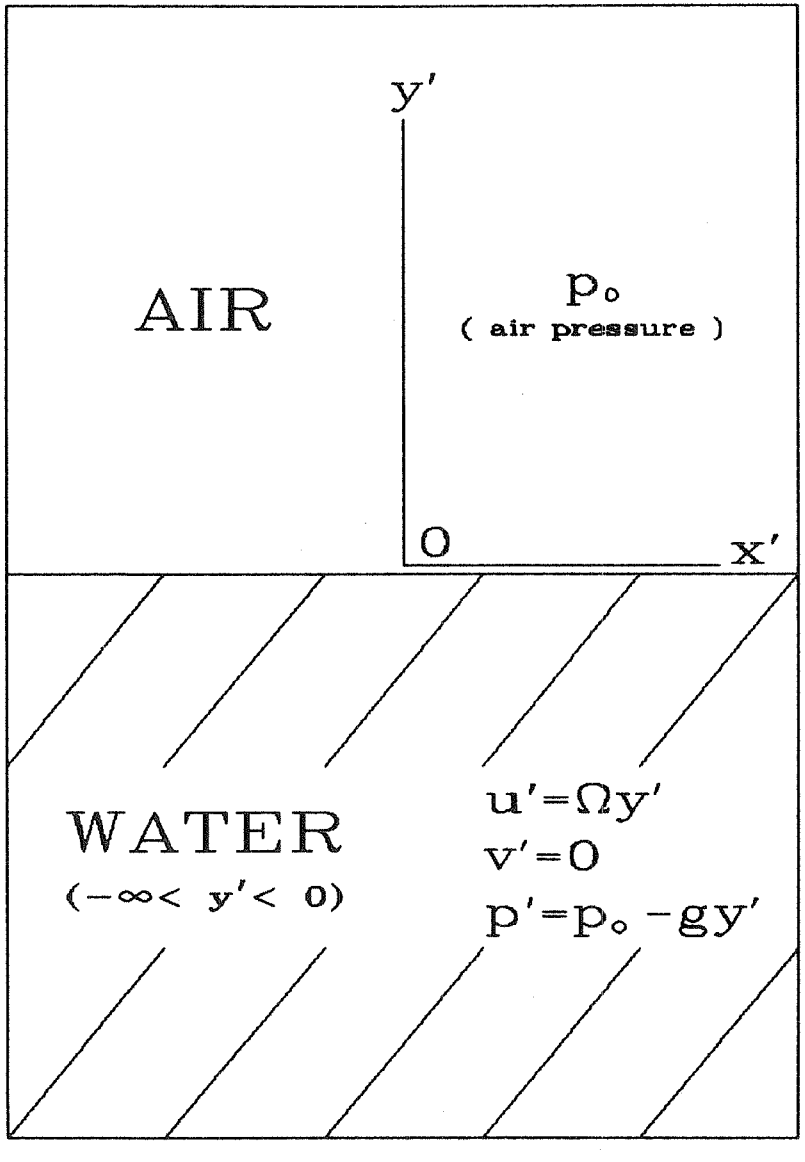


Figure 1-1

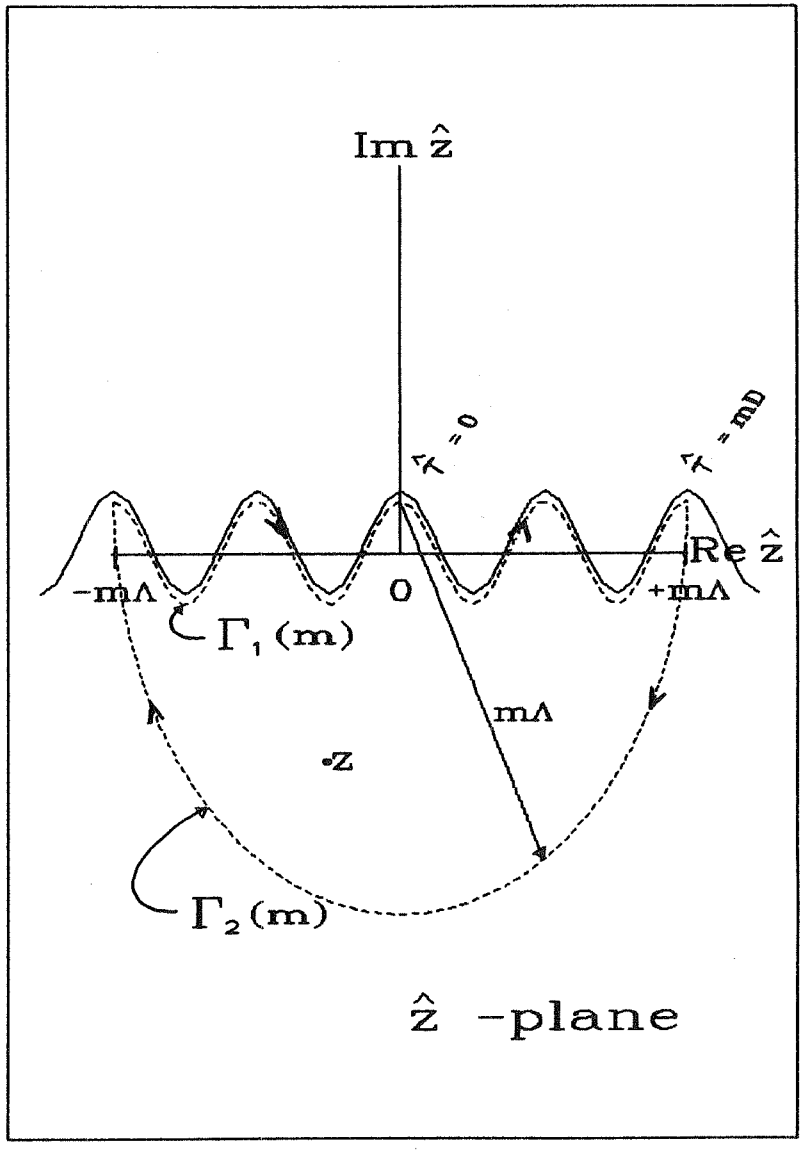


Figure 1-2

# CHAPTER 2

## VARIATIONAL PRINCIPLE AND SMALL AMPLITUDE WAVES

A variational principle for steady deep-water waves on a linear shear current is established. From this principle an average Lagrangian for small amplitude (Stokes-type) waves is constructed and then these waves are calculated to second order.

### 2.1. A variational principle

Consider the following variational principle:

$$\delta \int_R \int l \, dx' dt = 0 \quad ,$$

$$l = -\int_{-\infty}^{\eta'} \left\{ \frac{\partial \varphi'}{\partial t} + \frac{1}{2}\left[\nabla' \varphi'\right]^2 + \Omega y' \frac{\partial \varphi'}{\partial x'} \right\} dy' - \frac{1}{6}\Omega^2 \eta'^3 + \frac{1}{2}\left[\Omega c - g\right]\eta'^2 + \Omega \psi_0 \eta' \tag{2.1.1}$$

where $\varphi'(x', y', t)$ is the potential in the original $(x', y')$ coordinate system, $\eta'(x', t)$ is the surface elevation, and $R$ is an arbitrary region in $(x', t)$ space.

For infinitesimal changes $\delta\varphi'$ in $\varphi'$ after application of the chain rule, and integration by parts,

$$-\delta \int_R \int l \, dx' dt =$$

$$\int_R \int \left\{ \frac{\partial}{\partial t} \int_{-\infty}^{\eta'} \delta\varphi' \, dy' + \frac{\partial}{\partial x'} \int_{-\infty}^{\eta'} \left[ \frac{\partial \varphi'}{\partial x'} \delta\varphi' + \Omega y' \, \delta\varphi' \right] dy' \right\} dx' \, dt$$

$$-\int_R \int \int_{-\infty}^{\eta'} \left\{ \frac{\partial^2 \varphi'}{\partial x'^2} + \frac{\partial^2 \varphi'}{\partial y'^2} \right\} \delta\varphi' \, dy' \, dx' \, dt$$

$$-\int_R \int \left\{ \left[ \frac{\partial \eta'}{\partial t} + \frac{\partial \eta'}{\partial x'} \frac{\partial \varphi'}{\partial x'} + \Omega y' \frac{\partial \eta'}{\partial x'} - \frac{\partial \varphi'}{\partial y'} \right] \delta\varphi' \right\}_{y' = \eta'} dx' \, dt$$

$$-\int_R \int \left\{ \frac{\partial \varphi'}{\partial y'} \delta\varphi' \right\}_{y' = -\infty} dx' \, dt \quad .$$

Using Green's Theorem the first term can be written as an integral over the

boundary of $R$. By the usual arguments in the calculus of variations (see Luke (1967)), if the variational equation (2.1.1) is to hold true for all $\delta\varphi'$ it must be that

$$\nabla'^2\varphi' = 0 \tag{2.1.2a}$$

$$\frac{\partial\eta'}{\partial t} + \left[\frac{\partial\varphi'}{\partial x'} + \Omega y'\right]\frac{\partial\eta'}{\partial x'} = \frac{\partial\varphi'}{\partial y'} \quad \text{on} \quad y' = \eta'(x',t) \tag{2.1.2b}$$

$$\frac{\partial\varphi'}{\partial y'} \to 0 \quad \text{as} \quad y' \to -\infty \quad . \tag{2.1.2c}$$

For small variations $\delta\eta'$ in $\eta'$,

$$-\delta\int_R\int l\, dx'dt =$$

$$\int_R\int\left\{\left[\frac{\partial\varphi'}{\partial t} + \frac{1}{2}\left[\nabla'\varphi'\right]^2 + \Omega y'\frac{\partial\varphi'}{\partial x'}\right]_{y'=\eta'} + \frac{1}{2}\Omega^2\eta'^2 + \left[g - \Omega c\right]\eta' - \Omega\psi_0\right\}\delta\eta'\, dx'dt \quad .$$

Similarly if (2.1.1) is to be satisfied for all variations $\delta\eta'$ then

$$\frac{\partial\varphi'}{\partial t} + \frac{1}{2}\left[\frac{\partial\varphi'}{\partial x'}\right]^2 + \frac{1}{2}\left[\frac{\partial\varphi'}{\partial y'}\right]^2 + \Omega y'\frac{\partial\varphi'}{\partial x'} + \frac{1}{2}\Omega^2 y'^2 - \Omega c y' + g y' - \Omega\psi_0 = 0$$
$$\text{on} \quad y' = \eta'(x',t) \quad . \tag{2.1.2d}$$

Equations (2.1.2a) and (2.1.2b) are just (1.1.7) and (1.1.11) rewritten. (2.1.2c) is a slightly weaker form of (1.1.6). If steady waves are assumed then (2.1.2d) is the same as (1.1.10) with $\psi'$ replaced (from section 1.2) by

$$\psi' = -\frac{1}{2}\Omega y'^2 + c y' + \psi_0 \quad \text{on} \quad y' = \eta'(x',t) \quad .$$

In effect equations (2.1.2), which follow from the variational principle (2.1.1), are just the formulation for steady waves in the original $(x',y')$ coordinate system.

### 2.2. Small amplitude waves

Like Whitham (1967) we shall compute the Stokes-type waves by substituting the appropriate series expansions into the variational principle and obtaining the coefficients from the variational equations.

First the Fourier series

$$\eta'(x',t) = \sum_{n=1}^{\infty} a_n \cos n\vartheta$$

$$\varphi'(x',y',t) = \sum_{n=1}^{\infty} \frac{1}{n} A_n e^{nky'} \sin n\vartheta$$

are substituted into the average Lagrangian

$$L = \frac{1}{2\pi}\int_0^{2\pi} (-l)\, d\vartheta \quad .$$

For these steady, periodic and symmetric waves, $\vartheta$ is defined by $\vartheta = k(x'-ct)$ where the wavenumber $k = \frac{2\pi}{\lambda}$. Note that $\varphi'$ satisfies (2.1.2a) and (2.1.2c) already, and so the coefficients $A_n$ and $a_n$ are chosen to satisfy the wave surface conditions.

Plug the series for $\varphi'$ into $l$ and simplify this expression using the product formula for sines and cosines to arrive at

$$-l = -c\sum_{n=1}^{\infty} \frac{1}{n} A_n e^{nk\eta'} \cos n\vartheta + \tfrac{1}{2}k \sum_{n=2}^{\infty}\sum_{m=1}^{n-1} \frac{1}{n} A_m A_{n-m} e^{nk\eta'} \cos(n-2m)\vartheta$$
$$+ \Omega \sum_{n=1}^{\infty} \frac{1}{n} A_n \eta' e^{nk\eta'} \cos n\vartheta - \frac{1}{k}\Omega \sum_{n=1}^{\infty} \frac{1}{n^2} A_n e^{nk\eta'} \cos n\vartheta$$
$$+ \tfrac{1}{6}\Omega^2 \eta'^3 + \tfrac{1}{2}[g - \Omega c]\eta'^2 - \Omega\psi_0\eta' \quad .$$

In advance $a_n$ and $A_n$ are taken to be $O(a_1^n)$ for small amplitudes. $\eta'$ is replaced by its series and $L$ is computed up to and including $O(a_1^4)$ since the $O(a_1^4)$ terms contain the first nonlinear effects. After considerable algebra it is found that

$$L = -[\gamma_1 A_1 + \gamma_2 A_2] + \tfrac{1}{2}\gamma_{11}A_1^2 + \tfrac{1}{2}\gamma_{22}A_2^2 + \gamma_{12}A_1A_2 +$$
$$\tfrac{1}{4}[g - \Omega c][a_1^2 + a_2^2] + \tfrac{1}{8}\Omega^2 a_1^2 a_2 + O(a_1^6) \quad , \qquad (2.2.1)$$

where

$$\gamma_1 = ck[\tfrac{1}{2}a_1 + \tfrac{1}{4}k\, a_1a_2 + \tfrac{1}{16}k^2 a_1^3] - \Omega[\tfrac{1}{4}k\, a_1a_2 + \tfrac{1}{8}k^2 a_1^3]$$

$$\gamma_2 = ck\left[\tfrac{1}{2}a_2 + \tfrac{1}{4}k\,a_1^2\right] - \Omega\left[\tfrac{1}{8}k\,a_1^2\right]$$

$$\gamma_{11} = \tfrac{1}{2}k + \tfrac{1}{2}k^3 a_1^2$$

$$\gamma_{12} = \tfrac{1}{2}k^2 a_1$$

$$\gamma_{22} = \tfrac{1}{4}k \quad .$$

Here the average Lagrangian $L$ has been determined (to the order of our interest) in terms of $a_1$, $a_2$, $A_1$, and $A_2$. $a_1$ can be thought of as a fundamental parameter related to the waveheight. The other three coefficients are functions of $a_1$ and are found as solutions to the variational equations

$$\frac{\partial L}{\partial A_1} = 0 \quad , \quad \frac{\partial L}{\partial A_2} = 0 \quad , \quad \frac{\partial L}{\partial a_2} = 0 \quad .$$

If $L$ is written as a function of $a_1$ only, then the dispersion relation follows from

$$\frac{\partial L}{\partial a_1} = 0 \quad .$$

First we determine $A_1$ and $A_2$ in terms of $a_1$ and $a_2$ by solving the first two variational equations mentioned above. They are equivalent to the two linear relations

$$\gamma_{11}A_1 + \gamma_{12}A_2 = \gamma_1 \quad , \quad \gamma_{12}A_1 + \gamma_{22}A_2 = \gamma_2$$

which have as their solution

$$A_1 = \frac{\gamma_1\gamma_{22} - \gamma_2\gamma_{12}}{\gamma_{11}\gamma_{22} - \gamma_{12}^2} \quad , \quad A_2 = \frac{\gamma_2\gamma_{11} - \gamma_1\gamma_{12}}{\gamma_{11}\gamma_{22} - \gamma_{12}^2} \quad . \qquad (2.2.2)$$

$L$ may then be expressed in terms of $a_1$ and $a_2$ only. Using relations (2.2.2) and the preceding expressions for the $\gamma$'s , (2.2.1) becomes

$$L = -\tfrac{1}{4}\left[c^2k + \Omega c - g\right]a_1^2 + \tfrac{1}{16}k\left[c^2k^2 - \tfrac{1}{2}\Omega^2\right]a_1^4 +$$

$$\tfrac{1}{4}\left[c^2k^2 + 2\Omega ck + \tfrac{1}{2}\Omega^2\right]a_1^2 a_2 - \tfrac{1}{4}\left[2c^2k + \Omega c - g\right]a_2^2 + O(a_1^6) \quad . \qquad (2.2.3)$$

If we consider the variation of this new $L$ with respect to $a_1$, then the lowest order approximation gives the linear dispersion relation

$$c = c_0 + O(a_1^2) \quad \text{where} \quad c_0^2 k + \Omega c_0 - g = 0 \quad . \tag{2.2.4}$$

With this last relation (2.2.3) can be rewritten and then the variational equation $\frac{\partial L}{\partial a_2} = 0$ formed to yield a formula for $a_2$ in terms of $a_1$ which is

$$a_2 = \frac{1}{2c_0^2 k}[c_0^2 k^2 + 2\Omega c_0 k + \tfrac{1}{2}\Omega^2]a_1^2 + O(a_1^4) \quad . \tag{2.2.5}$$

After replacement of $a_2$ by this expression, the Lagrangian is finally simplified to

$$L = -\tfrac{1}{4}[c^2 k + \Omega c - g]a_1^2 +$$

$$\frac{1}{16c_0^2 k}\left(c_0^4 k^4 - \tfrac{1}{2}\Omega^2 c_0^2 k^2 + [c_0^2 k^2 + 2\Omega c_0 k + \tfrac{1}{2}\Omega^2]^2\right)a_1^4 + O(a_1^6) \tag{2.2.6}$$

Here $L$ is a function of $a_1$, $c$ and $k$ only and its substitution into the variational equation $\frac{\partial L}{\partial a_1} = 0$ yields the nonlinear dispersion relation

$$c^2 k + \Omega c - g =$$

$$\frac{1}{2c_0^2 k}\left(c_0^4 k^4 - \tfrac{1}{2}\Omega^2 c_0^2 k^2 + [c_0^2 k^2 + 2\Omega c_0 k + \tfrac{1}{2}\Omega^2]^2\right)a_1^2 + O(a_1^4) \quad . \tag{2.2.7}$$

If $\Omega = 0$ Stoke's result for irrotational waves is recovered; that is,

$$c^2 k - g = c_0^2 k^3 a_1^2 + O(a_1^4) \quad \text{where} \quad c_0^2 k = g \quad .$$

At this point we have found (to second order) the expansion for Stokes-type waves on a linear shear current. $c_0$, the lowest order approximation to the wave velocity $c$ is given by (2.2.4), while to higher order $c$ is found from the amplitude dependent relation (2.2.7). $a_2$ is determined by (2.2.5), and from the formulas (2.2.2) it can be deduced that

$$A_1 = c_0 a_1 + O(a_1^3)$$

$$A_2 = \frac{\Omega}{2c_0 k}[\Omega + 3c_0 k]a_1^2 + O(a_1^4) \quad .$$

The same procedure could be used to determine a higher order approximation; however, the algebra would be tedious.

# CHAPTER 3

# EXTREME WAVES

In this chapter we argue that, independent of $\Omega$, if the slope of a steady wave profile has a simple discontinuity at a crest (which means that this crest has a corner), then the included angle must be $\frac{2\pi}{3}$ radians. Although Miche (1944) has shown that this result holds for rotational flows in general, for completeness we present (for the linear shear case) a simple argument similar to that of Stokes (1847). Stokes was the first to consider these waves with sharp crests, which shall be called extreme waves; however, for the most part he confined his attention to $\Omega = 0$. Amick, Fraenkel and Toland (1982) have recently given the rigorous proof that for $\Omega = 0$ this extreme wave does exist; although they have not yet shown that it is also the wave of greatest height. This indicates a likelihood that for $\Omega \neq 0$ extreme waves also exist.

## 3.1. An argument for $120^\circ$ corners

In this section the local behavior of both the wave profile and the complex function $w(z)$ is ascertained. Recall from section 1.3 the definitions that $w(z) \equiv \varphi(x,y) + i\,\psi(x,y)$ and $z = x + iy$, where $(x,y)$ are the space coordinates in the steady frame of reference.

Allowing for certain singularities at the sharp crest, we assume

$$w(z) = \sum_{n=0}^{\infty} R_n (z - z_0)^n + R\,(z - z_0)^b + o(|z - z_0|^b) \quad \text{as} \quad z \to z_0 \qquad (3.1.1)$$

where the unknown $b$ is some real number excluding the non-negative integers, and $z_0 = x_0 + iy_0$ is the position of the crest. Insisting on a continuous velocity field, we must have that a crest with a corner is a stagnation point in this steady frame. A mathematical statement of this is

$$\frac{dw}{dz}(z_0) + \Omega y_0 - c = 0 \quad , \tag{3.1.2}$$

which for the function $q(\tau)$ used in sections (1.3)-(1.4) implies that

$$q = 0 \quad \text{at} \quad z = z_0 \quad . \tag{3.1.3}$$

Substitution of (3.1.1) into equation (3.1.2) with the assumption that $\frac{d}{dz}$ of the o-term is $o(|z - z_0|^{b-1})$ leads to the restriction that $b > 1$ and $R_1 = c - \Omega y_0$.

If polar coordinates are introduced by $z - z_0 = \rho e^{i\theta}$ with $-\pi < \theta \leq \pi$ and $\rho > 0$, then the Re part of (3.1.1) becomes

$$\varphi = \sum_{n=0}^{\infty} r_n \rho^n \cos(n\theta + \chi_n) + r\rho^b \cos(b\theta + \chi) + o(\rho^b) \quad \text{as} \quad \rho \to 0 \quad . \tag{3.1.4}$$

Here it has been supposed that $R_n = r_n e^{i\chi_n}$ (and $R = r e^{i\chi}$) with $-\pi < \chi_n \leq \pi$ and $r_n > 0$. For waves moving to the right ($c > 0$), observe that $R_1 = c - \Omega y_0$ implies

$$r_1 = c - \Omega y_0 \tag{3.1.5a}$$

$$\chi_1 = 0 \quad . \tag{3.1.5b}$$

If in our polar coordinates $\theta = \Theta(\rho)$ describes the wave profile, then locally the extreme wave is given by

$$\Theta(\rho) = \theta_c \pm \delta + o(1) \quad \text{as} \quad \rho \to 0 \quad . \tag{3.1.6}$$

The + sign is chosen if $\rho \to 0$ from the side with $x > x_0$ ; similarly, the - sign is picked if the approach is made with $x < x_0$. The ray $\theta = \theta_c$ bisects the angle at the crest and $2\delta$ is the measure of the included angle. Using the coordinate transformation $x = x_0 + \rho\cos(\theta)$ and $y = y_0 + \rho\sin(\theta)$, we can rewrite the dynamic boundary condition (1.2.4b) in terms of the polar coordinates. Now in order that $\varphi$ given by (3.1.4) satisfies this condition as $\rho \to 0$ (from both sides), it becomes necessary that $\theta_c = -\frac{\pi}{2}$ and

$$\tfrac{1}{2}r^2 b^2 \rho^{2b-2} + g\, y_0 - g\,\rho\cos\delta + o(\rho^{2b-2}) = B \quad \text{as} \quad \rho \to 0 \quad . \quad (3.1.7)$$

Here (3.1.5) and (3.1.6) have been used. The implications of relation (3.1.7) are

$$b = \tfrac{3}{2}$$

$$g\, y_0 = B$$

$$\tfrac{1}{2}r^2 (\tfrac{3}{2})^2 = g\cos\delta \quad .$$

This value of $b$ suggests that $\frac{dw}{dz}$ has a square - root branch point at the sharp crest of the extreme wave.

We still need to determine $\delta$ and do so by forcing $\varphi$ to locally satisfy the kinematic boundary condition (1.2.4c). With $b = \frac{3}{2}$ and $\theta_c = -\frac{\pi}{2}$ this condition will require that the two equations

$$\left\{\tfrac{3}{2}r\,\rho^{\frac{1}{2}}\cos(-\tfrac{\pi}{4} \pm \tfrac{\delta}{2} + \chi) + o(\rho^{\frac{1}{2}})\right\}\left\{\pm\cot\delta + o(1)\right\}$$

$$= \tfrac{3}{2}r\,\rho^{\frac{1}{2}}\sin(-\tfrac{\pi}{4} \pm \tfrac{\delta}{2} + \chi) + o(\rho^{\frac{1}{2}}) \quad (3.1.8)$$

be satisfied as $\rho \to 0$. Again the choice of sign depends on whether $\rho$ approaches zero from the left or the right. One choice of sign implies that

$$\cos(+\tfrac{3}{2}\delta - \tfrac{\pi}{4} + \chi) = 0 \quad .$$

Likewise, the other choice gives

$$\cos(-\tfrac{3}{2}\delta - \tfrac{\pi}{4} + \chi) = 0 \quad .$$

The solution of these two equations is $\delta = \frac{\pi}{3}$ and $\chi = -\frac{3\pi}{4}$ (for waves moving to the right). Thus, the included angle, $2\delta$, is $\frac{2\pi}{3}$.

The dynamic boundary equation has been satisfied as $\rho \to 0$ for terms up to $O(\rho)$. This can be seen in (3.1.7) if $b$ is replaced by $\frac{3}{2}$. Because $b = \frac{3}{2}$, the

next higher order terms in this equation would be $O(\rho^{\frac{3}{2}})$ and not $O(\rho^2)$. If we wish to satisfy the boundary condition to this next order then it becomes clear that we must include a term $O(\rho^{\frac{1}{2}})$ in our polar description of the wave profile. Substitution of (3.1.4) and

$$\Theta(\rho) = \theta_c \pm (\delta + S\rho^{\frac{1}{2}}) + o(\rho^{\frac{1}{2}}) \quad \text{as} \quad \rho \to 0 \tag{3.1.9}$$

into (1.2.4b) and (1.2.4c) followed by collection of $O(\rho^{\frac{3}{2}})$ terms and $O(\rho)$ terms, respectively, shows after some work that

$$S = \tfrac{1}{3}\Omega g^{-\frac{1}{2}} \quad . \tag{3.1.10}$$

$R_2 = \frac{5}{12}\Omega i$ also comes out of the algebra. For waves with $c > 0$, (3.1.9) and (3.1.10) tell us how the curvature of the extreme wave near the crest depends upon the sign and magnitude of the shear parameter $\Omega$.

# CHAPTER 4

# NUMERICAL METHOD

In chapter 2 the behavior of small amplitude waves is determined. On the other end of the waveheight spectrum, the large amplitude "extreme" waves are studied in chapter 3.

In this chapter we discuss the method used to construct solutions for those intermediate waveheights, the missing link in the global picture. In many ways this middle region turns out to be the most interesting. Purely analytical means fail here and so we must turn to numerical procedures at which time the preliminary analysis in chapter 1 becomes invaluable. There the problem of determining a function of two space variables ($x$ and $y$) is reformulated into that of finding a function of one variable ($\tau$). The numerical techniques for this latter class of problems are very well understood, and for a given accuracy require less computer memory and time.

## 4.1. Peliminaries

We first point out that the parametrization in $\tau$ is a natural choice if we hope to solve for both near extreme waves and the extreme waves themselves.

Consider the parametrization in arclength $s$, where $s = 0$ corresponds to the wave crest ($\tau = 0$). For a fixed $\Omega$ focus on the wave profile as a function of $s$ and waveheight $h$ so that $\zeta = \zeta(s,h)$. If $h_e$ defines the waveheight of the extreme wave then we are interested in the limit $h \to h_e$. Although it seems likely that $\zeta(s,h) \to \zeta(s,h_e)$ uniformly in $s$ as $h \to h_e$, it cannot be the case that $\frac{d\zeta}{ds}(s,h) \to \frac{d\zeta}{ds}(s,h_e)$ uniformly in $s$. The argument follows by taking $s = 0$ and showing that as $h \to h_e$ it is impossible for $\frac{d\zeta}{ds}(0,h) \to \frac{d\zeta}{ds}(0,h_e)$. This is

obvious since if $h \neq h_e$ then by symmetry and smoothness $\frac{d\zeta}{ds}(0,h) = 1 + 0i$, and if $h = h_e$ then by the jump in slope $\frac{d\zeta}{ds}(0,h_e) = \frac{1}{2}(\sqrt{3} \pm i)$.

On the other hand, the parametrization in $\tau$ is a "smoother" one. Using $\frac{d\zeta}{d\tau} = -Lq(\tau)\frac{d\zeta}{ds}$ (as $\frac{ds}{d\tau} = -Lq$), it is clear that if $h \neq h_e$ then $\frac{d\zeta}{d\tau}(0,h) = -Lq(0) + 0i$. Also, for extreme waves $q(0) = 0$ and therefore $\frac{d\zeta}{d\tau}(0,h_e) = 0$. In this case there is no jump in derivative for the extreme wave. Better yet, $\frac{d\zeta}{d\tau}(0,h) \to \frac{d\zeta}{d\tau}(0,h_e)$ as $h \to h_e$ and so it is possible that the limit of first derivatives is uniform in $\tau$. The parametrization in $\tau$ is not perfect though and it can be shown that $\frac{d^2\alpha}{d\tau^2}$ is discontinous at the crest of the extreme wave.

We need to numerically solve the nonlinear system of equations (1.4.3); but prior to this we enlarge the system by adding to it the equation

$$V = 2B - 2g\,\mathrm{Im}\,\zeta(0) \quad . \tag{4.1.1}$$

$V$ is a new variable which from (1.3.12) and (3.1.3) is shown to equal zero for extreme waves. The motivation for adding (4.1.1) is just that extreme wave solutions may then be isolated by setting $V = 0$.

Two procedures are adopted for finding numerical solutions to the new system of equations (1.4.3) and (4.1.1). For both of them $\Lambda$ and $g$ are fixed in advance (which fixes the length and time scales). The differences are that in one of them $\Omega$ and $h$ are given and approximate solutions for $\zeta(\tau)$, $c$, $B$, $L$ and $V$ are constructed; whereas in the other, the roles of $V$ and $h$ are interchanged. For both procedures the equations are discretized in the same way.

**4.2. Discretization**

In dealing with the numerical approximation to (1.4.3) and (4.1.1) it is convenient to use real functions. Therefore the equations are broken up into their real and imaginary components after $\zeta(\tau)$ is replaced by $\alpha(\tau) + i\beta(\tau)$. $\alpha$ and $\beta$ are then discretized by

$$\alpha_j = \alpha(\tau_j) \quad , \quad \beta_j = \beta(\tau_j) \qquad j = 1,...,N \tag{4.2.2}$$

where the $\tau_j$'s define a uniform mesh of $N$ points by

$$\tau_j = \pi \frac{j-1}{N-1} \qquad j = 1,...,N \quad . \tag{4.2.2}$$

Because of symmetry it is sufficient to work in the interval $0 \leq \tau \leq \pi$.

Derivatives in our equations are replaced by sixth order centered finite differences except when extreme waves are calculated directly and then derivatives of $\alpha$ are replaced by one-sided differences at the first few points adjacent to the crest. Since $\frac{d^n\beta}{d\tau^n}$ does not jump at $\tau = 0$, centered differences remain accurate for $\beta$ derivatives at the crest.

Symmetry described by (1.4.3d) allows us to transform all integrals into new ones with the range of integration from $\hat{\tau} = 0$ to $\hat{\tau} = \pi$. The integrals are then replaced by sums using the trapezoidal rule since for uniform meshes and periodic integrands this is highly accurate. For the integro-differential equation (1.4.3a) L'Hospital's rule is applied to find the value of the integrand at the points where $\hat{\tau} = \tau$. This will introduce second order derivatives which are replaced by sixth order differences.

Discretization transforms the original problem into that of finding the solution to a nonlinear system of algebraic equations. Close examination reveals that (1.4.3a) provides $2N-2$ equations. Its real part at $\tau = \tau_j$ provides $N$ equations. On the contrary, its imaginary part yields only $N-2$ equations because at

$\tau = \tau_1$ ($\equiv 0$) and $\tau = \tau_N$ ($\equiv \pi$) identities result owed to the imposed symmetry. (1.4.3b) turns out one relation, and (1.4.3c) produces the constraint $\alpha_1 = 0$. The symmetry condition (1.4.3d) has already been used at all $\tau_j$ except $\tau_N$ to rewrite the integrals, etcetera. At $\tau_N$ its real part becomes $\alpha_N = \frac{1}{2}\Lambda$ but its imaginary part reduces to an identity. (1.4.3e), (1.4.3f) and (4.1.1) each contribute one more equation. (For class 1 waves which are defined in chapter 5, (1.4.3f) takes the simple form $h = \beta_1 - \beta_N$ if a crest is put at $\tau_1$.) In the end there are $2N+4$ equations. The counting is correct as the unknowns $\alpha_j$, $\beta_j$, $c$, $B$, $L$ and $V$ (or $h$ if $V$ is given) also total $2N+4$ in number.

We remark that for $\Omega = 0$ a shift in $y$-coordinate can be used to improve the accuracy of our scheme. If (1.4.3e) is replaced by $\int_0^{2\pi} \beta \, d\tau = 0$ then there are no derivatives to approximate in this new integral and the accuracy of the numerical approximation will increase. With this new relation (1.4.3b) simplifies to $4\pi BL = c\Lambda$ which is also better from a numerical standpoint. Fortunately, if $\Omega = 0$ the solutions to this new system are the same as those to the original one except that the new $\beta$ and $B$ are just shifted from the old ones. The shifted amounts are $\Delta y$ and $g\,\Delta y$, respectively, where $\Delta y = \frac{1}{\Lambda}\int_0^{2\pi} \beta \frac{d\alpha}{d\tau} d\tau$.

### 4.3. Newton's method and continuation

The nonlinear system of algebraic equations may be represented by

$$\vec{f}\,(\vec{\mu},\sigma) = 0 \tag{4.3.1}$$

where $\vec{\mu}$ is a vector whose components are the unknowns (the profile values at the mesh points, the wavespeed and so forth) and $\sigma$ represents one of the parameters ($h$, $V$ or $\Omega$) which are varied. This system is solved iteratively by Newton's method, represented by

$$J(\vec{\mu}_n,\sigma)\,\delta\vec{\mu}_n = -\vec{f}\,(\vec{\mu}_n,\sigma) \tag{4.3.2a}$$

$$\vec{\mu}_{n+1} = \vec{\mu}_n + \gamma\,\delta\vec{\mu}_n \tag{4.3.2b}$$

where $\gamma = 1$, $\vec{\mu}_n$ is the $n$th iterate, $J$ is the Jacobian matrix for $\vec{f}$, and $\vec{\mu}_0$ is a supplied first guess. $\delta\vec{\mu}_n$ is computed as the solution to the linear system (4.3.2a) by LU decomposition and then put in (4.3.2b) as the difference between old and new iterates. On occasion this method is replaced by its underrelaxed version in which $\gamma < 1$. This allows for a less accurate first guess, but then the convergence is only linear as opposed to quadratic for $\gamma = 1$.

If $\vec{\mu}(\sigma)$, the solution at $\sigma$, is already known and the solution at $\sigma + \delta\sigma$ is wanted, then a reasonable first guess for Newton's method at $\sigma + \delta\sigma$ is obtained by the one step Euler method

$$J(\vec{\mu}(\sigma),\sigma)\ \frac{d\vec{\mu}}{d\sigma} = -\frac{\partial\vec{f}}{\partial\sigma}(\vec{\mu}(\sigma),\sigma) \qquad (4.3.3a)$$

$$\vec{\mu}_0(\sigma+\delta\sigma) = \vec{\mu}(\sigma) + \delta\sigma\,\frac{d\vec{\mu}}{d\sigma}\ . \qquad (4.3.3b)$$

Using (4.3.3) in combination with (4.3.2) we can continue along in the parameter $\sigma$ and find solutions $\vec{\mu}(\sigma)$. If a solution curve folds (i.e., a limit point is encountered) then we switch parameters to follow it.

Simple bifurcation points occur between $\sigma$'s in which there is a sign change in the determinant of the Jacobian. Once these points are located more precisely by bisection then an approximation to the tangent of the new solution curve is either guessed (from known behavior) or estimated from the algebraic bifurcation equation. (See Keller (1977), for example.) With $\frac{d\vec{\mu}}{d\sigma}$ replaced by this tangent approximation, (4.3.3b) provides a first guess to a solution along this new branch. Newton's method pinpoints this solution and further continuation resolves the branch.

Our goal is to find both the region of solutions and the nature of them for a chunk of the $(h,\Omega)$ plane. To accomplish this continuations are made in several ways. The most useful one is to fix $\Omega$, start with a small amplitude wave given in

chapter 2 and continue up in the waveheight parameter $h$. As either folds or extreme waves are neared the continuation parameter is then switched to $V$ and varied towards zero, enabling continuation right up to the limiting wave. This isn't always successful because for some $\Omega$ there are gaps in $h$ where no solutions exist. Another helpful procedure is to fix $V = 0$ and vary $\Omega$, in this way resolving the extreme wave solutions in the $(h,\Omega)$ plane. Lastly, an alternate approach is to fix $h$ and vary $\Omega$.

After a wave is found numerically its integral properties are calculated from the discretized form of (1.5.4), (1.5.5) and (1.5.6). Additionally, for extreme waves the slope at the crest is computed using cubic splines.

### 4.4. Some checks

The results of any numerical calculation require verification and we use a series of checks. Small amplitude waves are compared with the predictions of weakly nonlinear theory in chapter 2. Included angles at the extreme wave crests are tested for their closeness to $120^{\circ}$. For $\Omega = 0$ the relation $B = \frac{1}{2}c^2$ serves as a check on accuracy, while for $\Omega \neq 0$ the relation $I = \psi_0 = \frac{1}{\Omega}(B - \frac{1}{2}c^2)$ provides the check. Perhaps the best overall test of accuracy, the results calculated on a given mesh are compared to those from a mesh with half the number of points. We also compare our results to those of others for specific values of the parameters.

# CHAPTER 5

# NUMERICAL RESULTS AND DISCUSSION

## 5.1. Definitions

Dimensionless quantities which are suitable for describing the results are given by

$$h^* = \frac{h}{\Lambda} \quad , \quad \Omega^* = \left(\frac{\Lambda}{2\pi g}\right)^{\frac{1}{2}} \Omega \quad , \quad c^* = \left(\frac{2\pi}{\Lambda g}\right)^{\frac{1}{2}} c \quad ,$$

$$T^* = \frac{1}{g}\left(\frac{2\pi}{\Lambda}\right)^2 T \quad , \quad P^* = \frac{1}{g}\left(\frac{2\pi}{\Lambda}\right)^2 P \quad , \quad I^* = g^{-\frac{1}{2}}\left(\frac{2\pi}{\Lambda}\right)^{\frac{3}{2}} I \quad .$$

Since $\Lambda = 2\pi$ and $g = 1$ in our actual computations, the $2\pi$ factors are introduced above to allow ease in converting to the dimensionless quantities.

We adopt the same terminology used by Chen & Saffman (1980). Any Stokes-type wave or its smooth continuation to finite amplitude defines a "regular" wave. All other waves are termed "irregular" waves. Recall from section 1.3 that wave profiles are computed in a window of horizontal length $\Lambda$. A regular wave having an integral multiple of wavelengths $n\lambda$ in this window is called a regular wave of class $n$. Irregular waves of class $n$ are bifurcations of these regular waves into waves having $n$ crests per wavelength.

Obviously all classes of regular waves are physically equivalent and the differences only occur in the description of them by the dimensionless variables above. In terms of these variables regular waves of class $n$ are related to regular waves of class 1 by

$$h_n^* = \frac{h_1^*}{n} \ , \ \Omega_n^* = n^{\frac{1}{2}} \Omega_1^* \ , \ c_n^* = \frac{c_1^*}{n^{\frac{1}{2}}} \ , \ T_n^* = \frac{T_1^*}{n^2} \ , \ P_n^* = \frac{P_1^*}{n^2} \ , \ I_n^* = \frac{I_1^*}{n^{\frac{3}{2}}} \ ,$$

where the subscript denotes the class.

## 5.2. Case of $\Omega^* = 0$

Since our method allows for accurate calculations in the region of the extreme wave, we pursue the irrotational case in order to improve upon and/or to verify the theoretical and numerical results of Longuet-Higgins & Fox (1978), Chen & Saffman (1980) and Rottman & Olfe (1980).

All computations are carried out in double precision on a Vax 11/750 computer and Newton's method is considered to have converged when the residuals are less than $10^{-11}$.

### 5.2.1. Regular waves

From section 5.1 it is sufficient to study only class 1 regular waves. We start with a small amplitude Stokes wave, continue first in waveheight and then in $V$ to a point near the extreme wave. This last wave is then used as a first guess in a direct calculation of the extreme wave. The calculations are done on both a mesh of 121 points per half wavelength and one of 61 points per half wavelength. Results from the two different meshes coincide to 8 significant figures for most amplitudes and to 5 significant figures for the near extreme waves. $B = \frac{1}{2}c^2$ checks to within an error of at worst $O(10^{-7})$. For each individual wave Newton's method takes 3 to 4 iterations to converge, which in CPU time is on the average about 9 minutes for a 61 point grid. Figure 5-1 shows a computational window one wavelength long with 5 different calculated profiles. Profile E) is the extreme wave which is computed to have $h^* = .141064$ and an included angle of $119.95^\circ$. Note that zero on the vertical axis represents the mean wave height level.

Figure 5-2 illustrates the manner in which mesh points uniformly spaced in $\tau$ automatically concentrate at the crest for extreme or near extreme waves. Notice that for a small amplitude wave as in A the grid is almost evenly spaced

along the profile.

Longuet-Higgins & Fox (1978) estimated that the value of $h^*$ for the extreme wave is .14107. They also predicted that the wavespeed and energies oscillate infinitely often as the extreme wave is approached through increasing waveheight. Figure 5-3 is a plot of wavespeed $c^*$ versus $h^*$ from our results. The inset shows a closeup of the region which borders the extreme wave and it seems to reveal the first relative maximum, the first relative minimum and possibly the second relative maximum of these wiggles. These oscillations decay so fast as a function of $h^*$ that it seems beyond the scope of double precision calculations to resolve many more of them. The weakly nonlinear approximation is also displayed in this figure and shown to be a pretty good approximation (at least visually) up to heights with $h^*$ about .03. Even for larger amplitudes the weakly nonlinear estimate is never all that bad; however, it is incapable of even roughly describing the behavior of the strongly nonlinear region close to the maximum waveheight. Figure 5-4 is a table of some important physical quantities for almost-extreme waves. It confirms the expected oscillations in energies. Furthermore it shows that our method works better than that of Chen & Saffman (1980) for this region, and it gives us an idea of the accuracy required to numerically resolve more details in it.

### 5.2.2. Irregular waves

There are no signs of bifurcation from class 1 regular waves to other symmetric waves. We allow for subharmonic bifurcations by considering class 2 regular waves. This time continuation in waveheight locates a simple bifurcation point at $h^* = .06446$ which agrees well with Chen & Saffman (1980). Continuation along this new branch of irregular class 2 waves leads up to a new extreme wave which is calculated directly. The same procedure is followed by starting with a class 3 regular wave. Continuation in height reveals a bifurcation point at

$h^* = .04294$. Following the new branch this time reveals two different irregular class 3 extreme waves. Figure 5-5 displays the bifurcation diagrams and the important profiles in these continuations. A and E are the points of bifurcation from regular to irregular waves. C, D and F are the calculated extreme waves, while B is just an intermediate point. In the class 2 case notice that the extreme wave profile C) has one sharp crest and one smooth one. This means that the regular wave A) has bifurcated into a wave with twice the wavelength. For class 3 one limiting wave has two sharp corners per wavelength and the other has only one. In either case the regular wave E) bifurcates into a wave of triple its original wavelength.

Rottman & Olfe (1980) used Michell's method to calculate irregular extreme waves directly. They concentrated on class 1 through class 4 and could only produce those waves having one sharp crest per wavelength. In order to completely compare the results of two different methods we also search for an irregular class 4 extreme wave. Since the regular to irregular wave bifurcation here is second order, the sign of the determinant of the Jacobian cannot be used to locate the bifurcation point. Nevertheless by estimating its location from a noticed pattern and using perturbed regular waves at that point as first guesses in Newton's method, we manage to jump onto an irregular class 4 branch. Again continuation and direct extreme wave calculation are employed to yield the limiting wave of interest. Figure 5-6 is a comparison of results for those extreme waves having one sharp crest per wavelength. Since in our method the $120^\circ$ corner at the crest is not an input as in Michell's method, we list the values of the included angles which are outputted. These angles hover close to $120^\circ$. Notice that our results are very close to those of Rottman & Olfe (1980). Our value of $h^* = .141064$ for the class 1 extreme wave is the most accurate so far and lies between the numbers quoted by Longuet-Higgins & Fox (1978) and Rott-

man & Olfe (1980).

Figure 5-7 has the computed profiles for the extreme waves that were just compared. Both regular and irregular class $n$ waves are shown in a window which in length is one wavelength of the irregular wave and $n$ wavelengths of the regular wave. It is interesting to note that the crests and troughs of irregular waves are slightly shifted horizontally from those of regular waves.

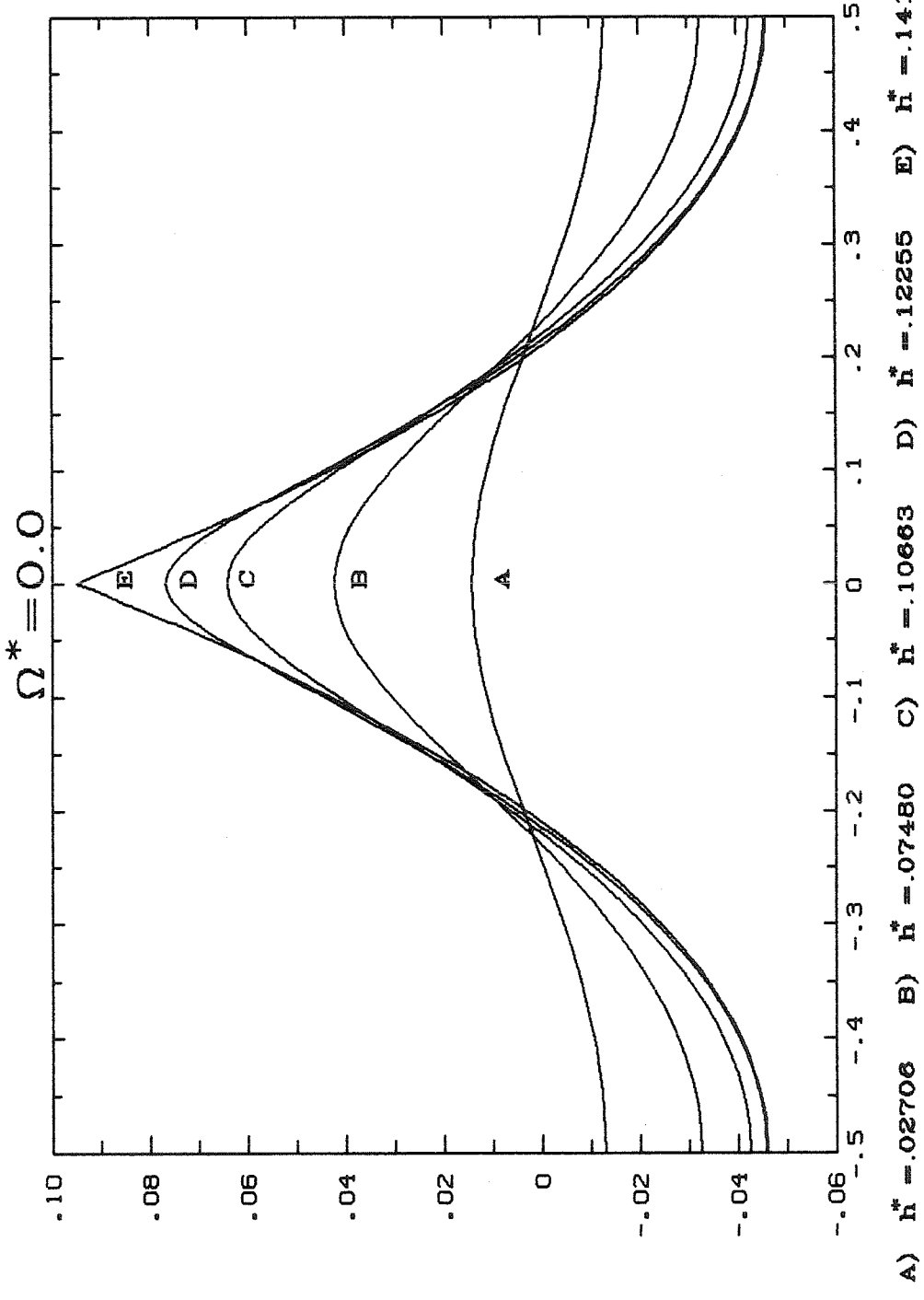
$\Omega^* = 0.0$
.10
.08
.06
.04
.02
0
-.02
-.04
-.06
-.5
-.4
-.3
-.2
-.1
0
.1
.2
.3
.4
.5
A
B
C
D
E
A) $h^* = .02706$ B) $h^* = .07480$ C) $h^* = .10663$ D) $h^* = .12255$ E) $h^* = .14106$

Figure 5-1

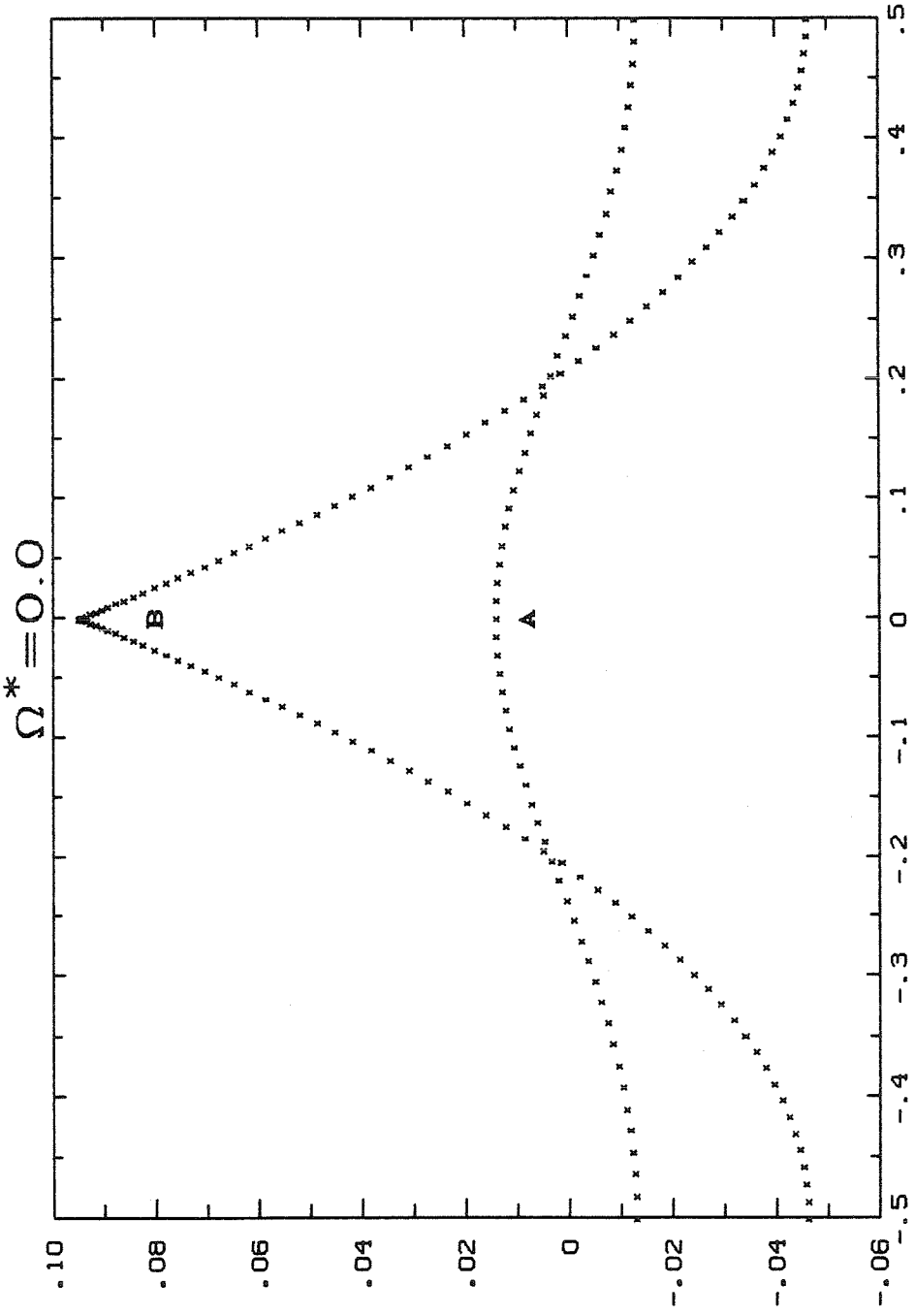
$\Omega^* = 0.0$
B
A
.10
.08
.06
.04
.02
0
-.02
-.04
-.06
-.5
-.4
-.3
-.2
-.1
0
.1
.2
.3
.4
.5
A) $h^* = .02706$
B) $h^* = .14106$

Figure 5-2

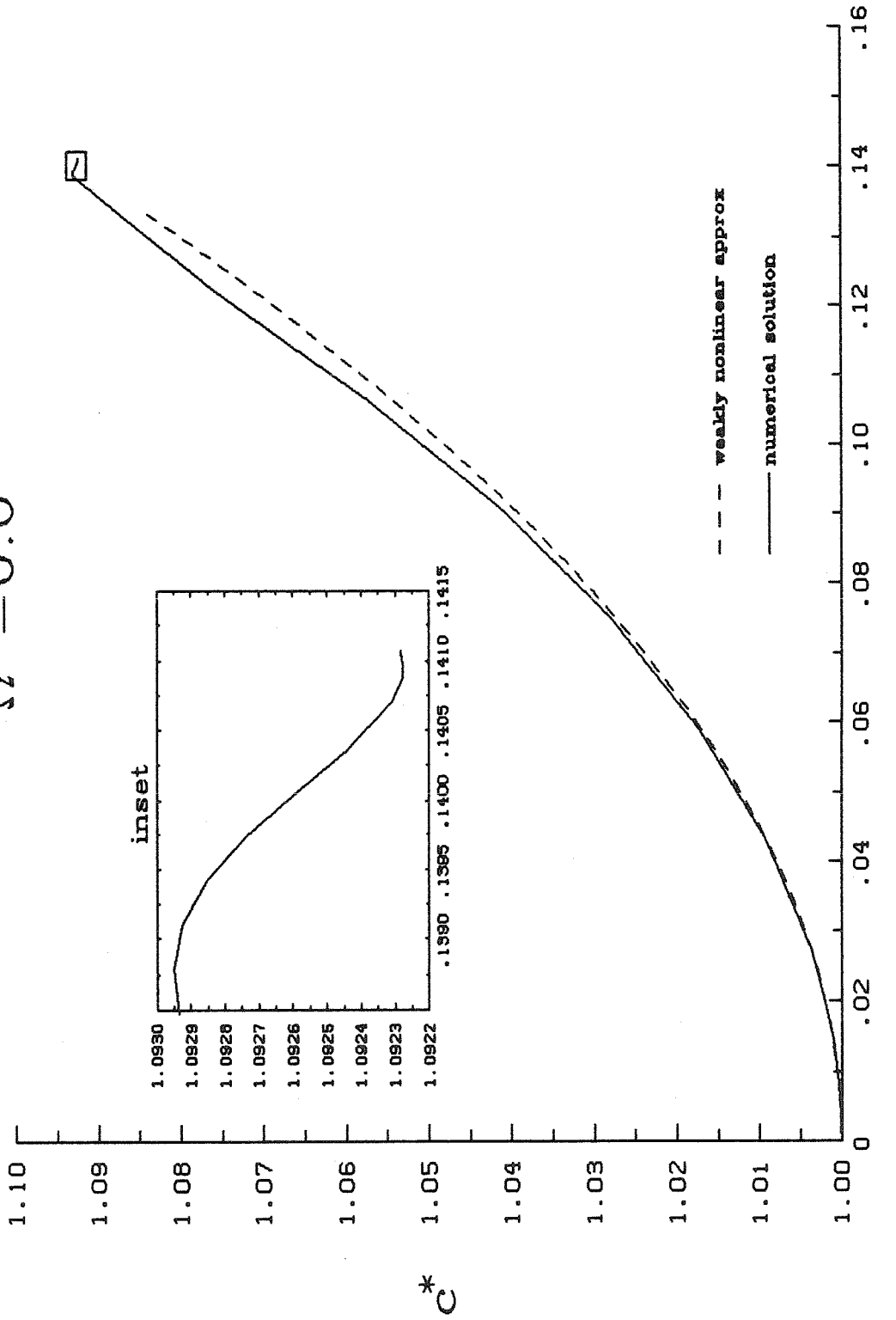
$\Omega^* = 0.0$
$c^*$
$h^*$
1.10
1.09
1.08
1.07
1.06
1.05
1.04
1.03
1.02
1.01
1.00
0
.02
.04
.06
.08
.10
.12
.14
.16
inset
1.0930
1.0929
1.0928
1.0927
1.0926
1.0925
1.0924
1.0923
1.0922
.1390
.1395
.1400
.1405
.1410
.1415
weakly nonlinear approx
numerical solution

Figure 5-3

## PROPERTIES OF THE ALMOST EXTREME WAVE FOR $\Omega^*=0.0$
(regular class 1 waves)

| $h^*$ | $c^*$ | $T^*$ | $P^*$ | $I^*$ |
|---|---|---|---|---|
| .136873 | 1.092311 | .038877 | .035152 | .071184 |
| .137987 | 1.092832 | .038815 | .035053 | .071037 |
| .138465 | 1.092934 | .038748 | .034979 | .070907 |
| .138783 | 1.092951 | .038689 | .034918 | .070797 |
| .139101 | 1.092924 | .038620 | .034851 | .070672 |
| .139420 | 1.092852 | .038542 | .034779 | .070536 |
| .139738 | 1.092735 | .038461 | .034706 | .070395 |
| .140056 | 1.092587 | .038384 | .034639 | .070263 |
| .140350 | 1.092442 | .038326 | .034591 | .070165 |
| .140690 | 1.092310 | .038288 | .034562 | .070105 |
| .140874 | 1.092278 | .038286 | .034562 | .070103 |
| .140969 | 1.092278 | .038289 | .034566 | .070109 |
| .141017 | 1.092282 | .038292 | .034568 | .070113 |
| .141041 | 1.092284 | .038292 | .034568 | .070114 |
| .141058 | 1.092285 | .038292 | .034568 | .070114 |
| .141064 | 1.092285 | .038292 | .034568 | .070114 |

Figure 5-4

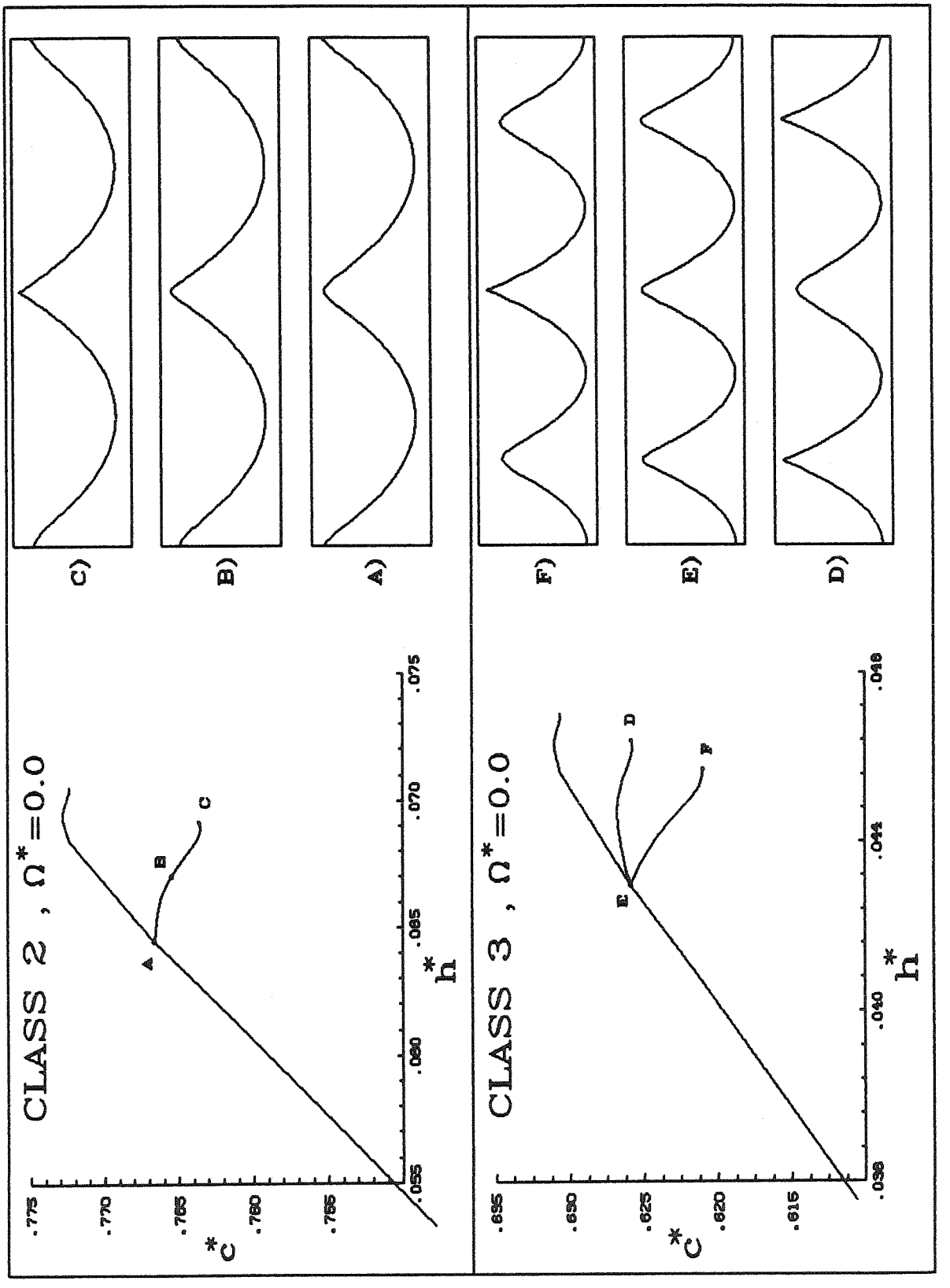


Figure 5-5

# COMPARISON OF RESULTS:
# EXTREME WAVE PROPERTIES FOR $\Omega^*=0.0$

| | $h^*$ | $c^*$ | $T^*$ | $P^*$ | $I^*$ | crest angle |
|---|---|---|---|---|---|---|
| REGULAR CLASS 1 CHEN & SAFFMAN (1980) | .14087 | 1.0923 | .03830 | .03457 | | |
| ROTTMAN & OLFE (1980) | .14106 | 1.0923 | .03829 | .03457 | | |
| PRESENT WORK | .141064 | 1.092285 | .038292 | .034568 | .070114 | 119.95° |
| IRREGULAR CLASS 2 CHEN & SAFFMAN (1980) | .06862 | .7637 | .008675 | .007955 | | |
| ROTTMAN & OLFE (1980) | .06907 | .7635 | .008661 | .007945 | | |
| PRESENT WORK | .06910 | .7635 | .008663 | .007946 | .02269 | 120.05° |
| IRREGULAR CLASS 3 CHEN & SAFFMAN (1980) | .04545 | .6210 | .003719 | .003430 | | |
| ROTTMAN & OLFE (1980) | .04575 | .6210 | .003716 | .003427 | | |
| PRESENT WORK | .04575 | .6210 | .03719 | .003431 | .01200 | 120.09° |
| IRREGULAR CLASS 4 ROTTMAN & OLFE (1980) | .03417 | .5367 | .002052 | .001898 | | |
| PRESENT WORK | .03419 | .5368 | .002055 | .001901 | .007658 | 120.15° |

Figure 5-6

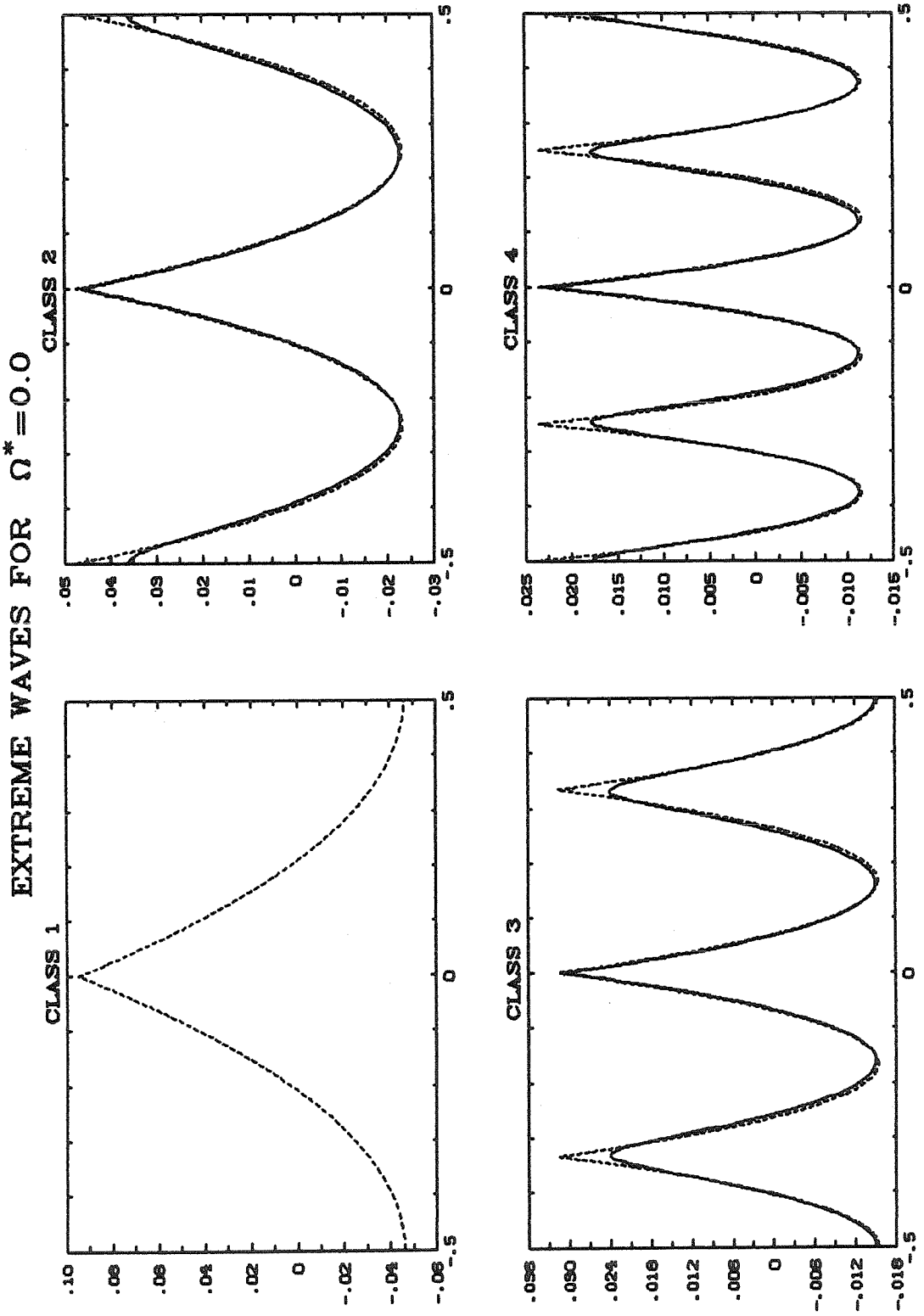
EXTREME WAVES FOR Ω*=0.0
CLASS 1
CLASS 2
CLASS 3
CLASS 4
regular wave
irregular wave

Figure 5-7

### 5.3. Case of $\Omega^* \neq 0$

With the introduction of vorticity into the problem some rather fascinating behavior is observed. Although for $\Omega^* = 0$ it seems that regular waves are unique if irregular waves are discounted, this is no longer necessarily true for waves on a linear shear current. (By "unique" we mean in the sense that given the wavelength, height and propagation direction there exists only one wave.) Furthermore, while it seems evident that for $\Omega^* = 0$ the extreme wave is the wave of greatest height this is not true for some $\Omega^* < 0$.

Recall that without loss of generality we consider waves moving only to the right so that $c^* > 0$.

#### 5.3.1. Regular waves

First we fix $\Omega^* = +1$. We begin with a small amplitude Stokes-type wave and then continue in waveheight and $V$ up to and including the extreme wave. Calculations on the 61 points per half wavelength grid and the 121 points one coincide to 6 significant digits or better. $B = \frac{1}{2}c^2 + \Omega I$ checks to within an error of at worst $O(10^{-8})$. Figure 5-8 displays 9 profiles in the order in which they appear in the continuation process. I) is the extreme wave profile shown to have a corner which is computed to include an angle of about 119°. The curvature of this wave at the crest differs from that of the $\Omega^* = 0$ regular extreme wave and this checks with the prediction of (3.1.9) and (3.1.10). Notice that the maximum allowable waveheight here is noticeably less than that for the irrotational case.

The same continuations are done for other positive $\Omega^*$. The curvature at the extreme wave becomes more noticeable and the maximum waveheight becomes less as $\Omega^*$ is increased. Figure 5-9 is a typical example of wavespeed versus waveheight for positive $\Omega^*$. Like the irrotational case $c^*$ is not monotonically increasing. For this particular illustration with $\Omega^* = +2$ the weakly non-

linear approximation appears visually accurate for $h^*$ up to about one third of the maximum height.

Next fix $\Omega^* = -1$. The profiles in figure 5-10 are calculated by continuing from a small amplitude wave in A) up to the extreme wave in I). It is discovered that at the sharp crest the included angle is close to 120° but the curvature there is opposite to that of positive $\Omega^*$. This time the maximum waveheight is larger than that of $\Omega^* = 0$.

Figure 5-11 is a table of calculated physical quantities as a function of $\Omega^*$ for regular extreme waves. One of its implications is that for waves moving to the right, negative shear ($\Omega^* < 0$) favors larger amplitudes than positive shear. Also as predicted, the included angle at the sharp crest is shown to be independent of $\Omega^*$ (to within a small error).

For more negative shear something new develops. The profiles pertaining to $\Omega^* = -1.6$ are found in figure 5-12. Observe that as we continue through these solutions the waveheight at first increases, then decreases and finally increases again as the limiting wave is neared. In other terms a fold exists if $h^*$ is the parameter, and waves are no longer unique for certain waveheights. The extreme wave which now has noticeable curvature at the corner is no longer the wave of greatest height. A further development of the continuation is that a bulge in the wave profile appears and then subsides.

The question naturally arises as to what happens to this bulge for even more negative shears. Part of the answer to this is in figure 5-13 where our results for $\Omega^* = -1.74$ are presented. In this case continuation from small amplitude only gets as far as wave D) where the profile almost touches itself. Beyond this point Newton's method diverges. Now we work backwards. The extreme wave for $\Omega^* = -1.74$ is located by fixing $V = 0$ and continuing down in $\Omega^*$ from the irrotational extreme wave. From this new wave we continue back

towards smaller amplitude waves. Again a point is reached where the iterative method diverges and this time it happens just after profile E), which also almost crosses itself, is computed. We summarize this result by saying that in the continuation from wave A) to I) a gap is found to exist between two "touching" waves D) and E), and within this gap there is no physical solution. Note that each touching wave is a limiting wave that encloses a bubble. A similar phenomenon occurs in capillary waves.

Perhaps the best means of describing this behavior more completely is figure 5-14. Here wavespeed versus waveheight is plotted for several values of $\Omega^*$. It is immediately obvious that the extreme wave height increases as $\Omega^*$ becomes more negative. We can see that the fold develops somewhere in $-1.5 < \Omega^* < -1.3$ and increases in size as $\Omega^*$ decreases. For a given $\Omega^*$ having such a fold there are values of $h^*$ where as many as two or three different waves exist. It is apparent from this diagram that for $\Omega^*$ more negative than approximately $-1.5$ the extreme wave is not the highest wave. Furthermore, the gap in solutions appears around $\Omega^* = -1.7$ and gets larger as $\Omega^*$ becomes more negative.

To further verify this behavior some numerical computations for $\Omega^* = -2$ are run. In figures 5-15 and 5-16 are graphed the profiles and the curve $c^*$ versus $h^*$, respectively. As before in the continuation from small amplitudes a limiting wave D) is discovered to mark the beginning of a gap. Across the gap is another limiting wave E) which encloses a larger bubble. As we continue through a fold the profiles become less bulging and finally a limiting wave I) with a corner is reached. From figure 5-16 it is seen that for waveheights less than maximum there are values of $h^*$ where either two, one or no solutions exist. When $\Omega^* = -2$ the larger waveheight calculations for the 121 and 61 point meshes coincide to 4 significant digits only, and the error in $B = \frac{1}{2}c^2 + \Omega I$ is

usually $O(10^{-5})$.

From our weakly nonlinear theory there are no signs of a critical value in $\Omega^*$ beyond which solutions fail to exist, and hence we believe that as $\Omega^* \to \pm\infty$ the limiting curves will never cross $h^*=0$. Figure 5-17 is a plot of the limiting curves in the $(h^*,\Omega^*)$ plane and it supports this belief. It also hints that the extreme wave will become the wave of greatest height again if $\Omega^*$ is slightly more negative than $-2.0$. This gets confirmed. Here it is appropriate to mention that as $|\Omega^*|$ is increased our numerical method becomes more sensitive and less accurate.

### 5.3.2. Irregular waves

Recall that for $\Omega^*=0$ bifurcations of regular class $n$ waves yield irregular class $n$ waves if $n > 1$. The same is true if $\Omega^* \neq 0$. For a given $\Omega^*$ these irregular wave branches can be resolved as before by first locating the bifurcation point in the regular wave branch. Figure 5-18 is a list of some calculated bifurcation points for class 2 and class 3 with $\Omega^*$ between $-1$ and $+1$.

We choose to confine our attention to extreme waves. $V=0$ is fixed and continuation is done in $\Omega^*$ starting from the irregular extreme waves of $\Omega^*=0$. In this way irregular extreme waves of $\Omega^* \neq 0$ are computed. Figure 5-19 shows the resultant paths in the $(h^*,\Omega^*)$ plane for class 2 and class 3. In figure 5-20 the profiles for $\Omega^*=\pm 1$ are given. The curvature at the crest is the most noticeable difference between positive and negative $\Omega^*$.

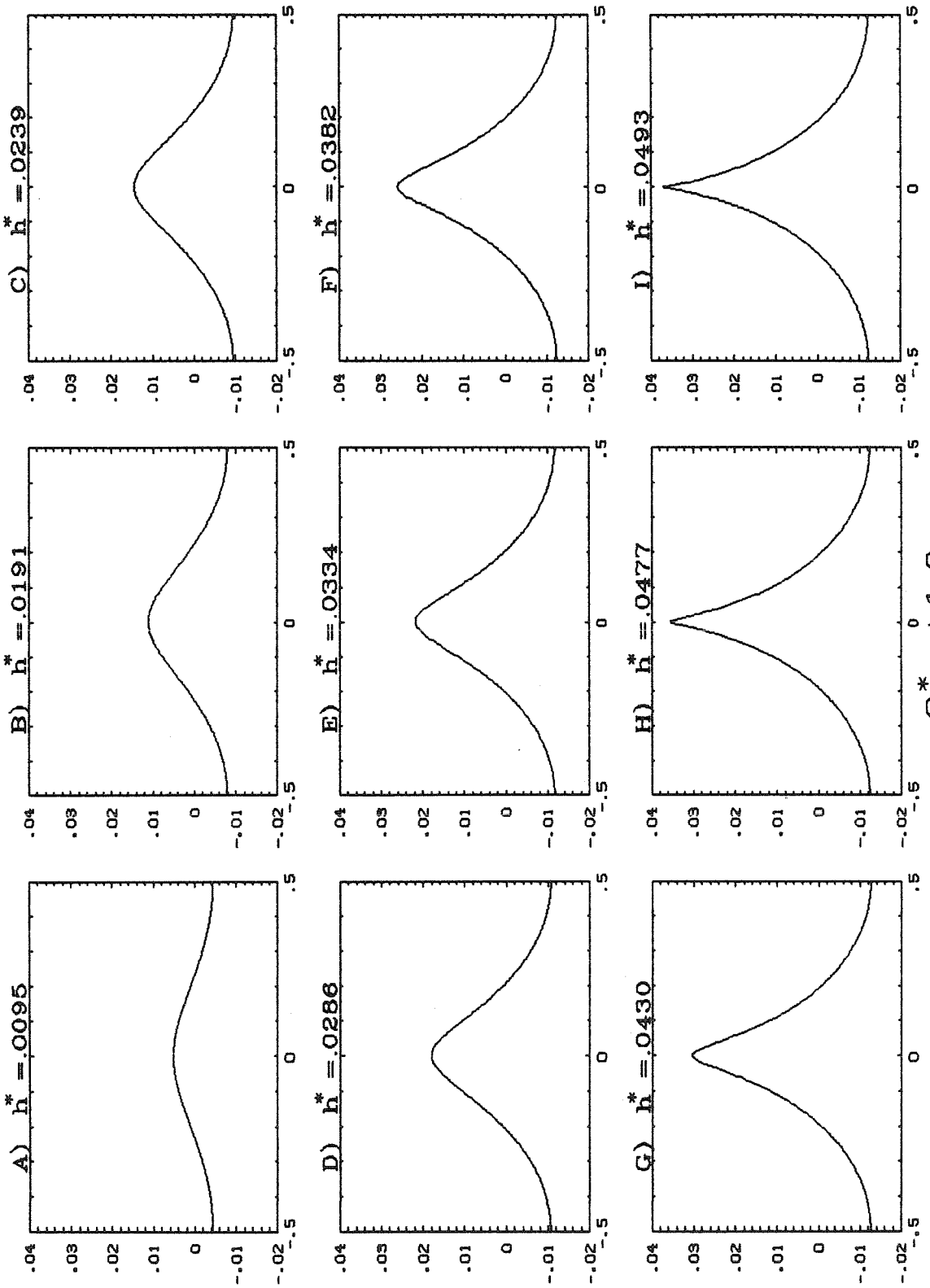
A) h* =.0095
B) h* =.0191
C) h* =.0239
D) h* =.0286
E) h* =.0334
F) h* =.0382
G) h* =.0430
H) h* =.0477
I) h* =.0493
Ω* = +1.0

Figure 5-8

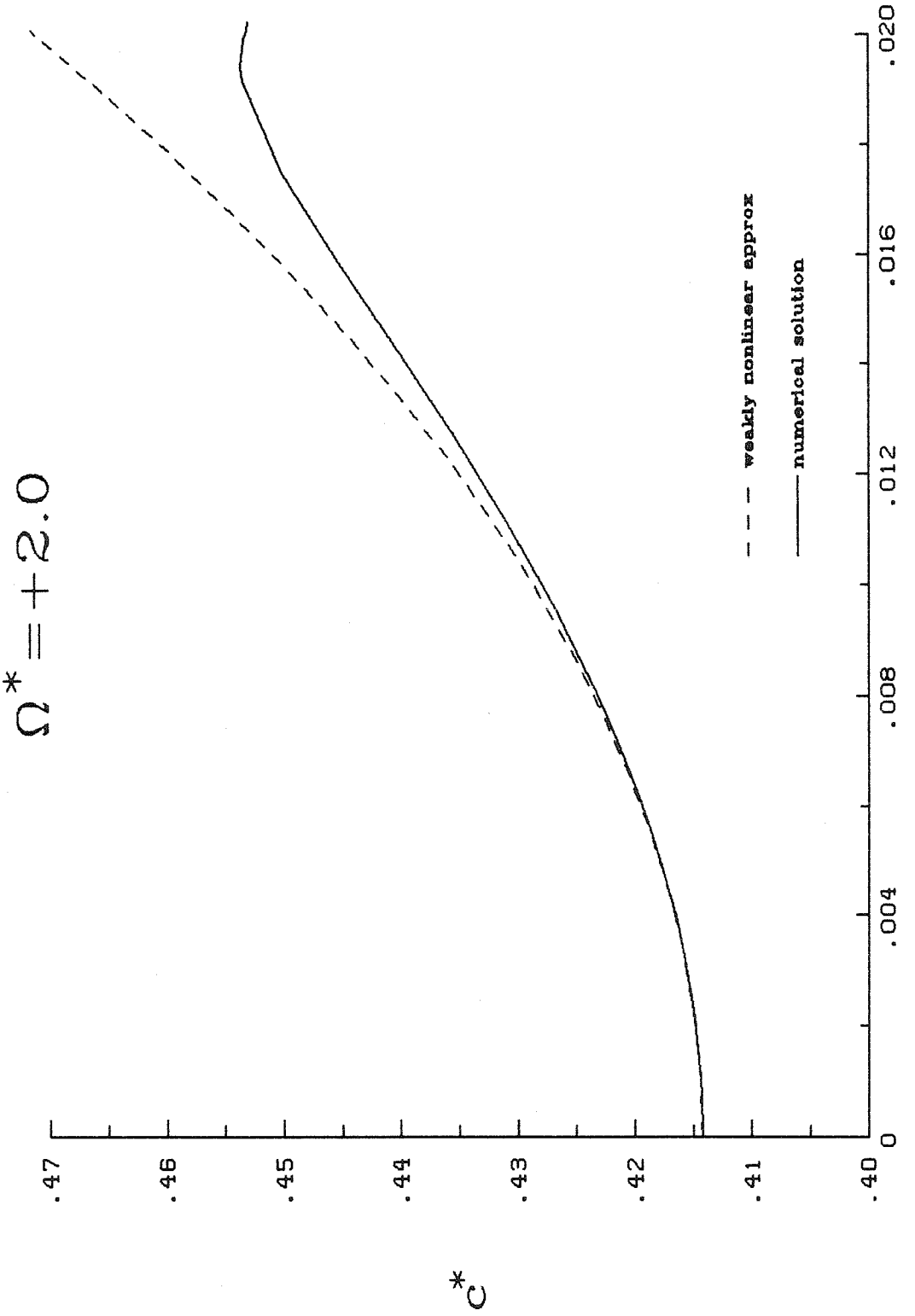
$\Omega^* = +2.0$
$c^*$
$h^*$
.47
.46
.45
.44
.43
.42
.41
.40
0
.004
.008
.012
.016
.020
weakly nonlinear approx
numerical solution

Figure 5-9

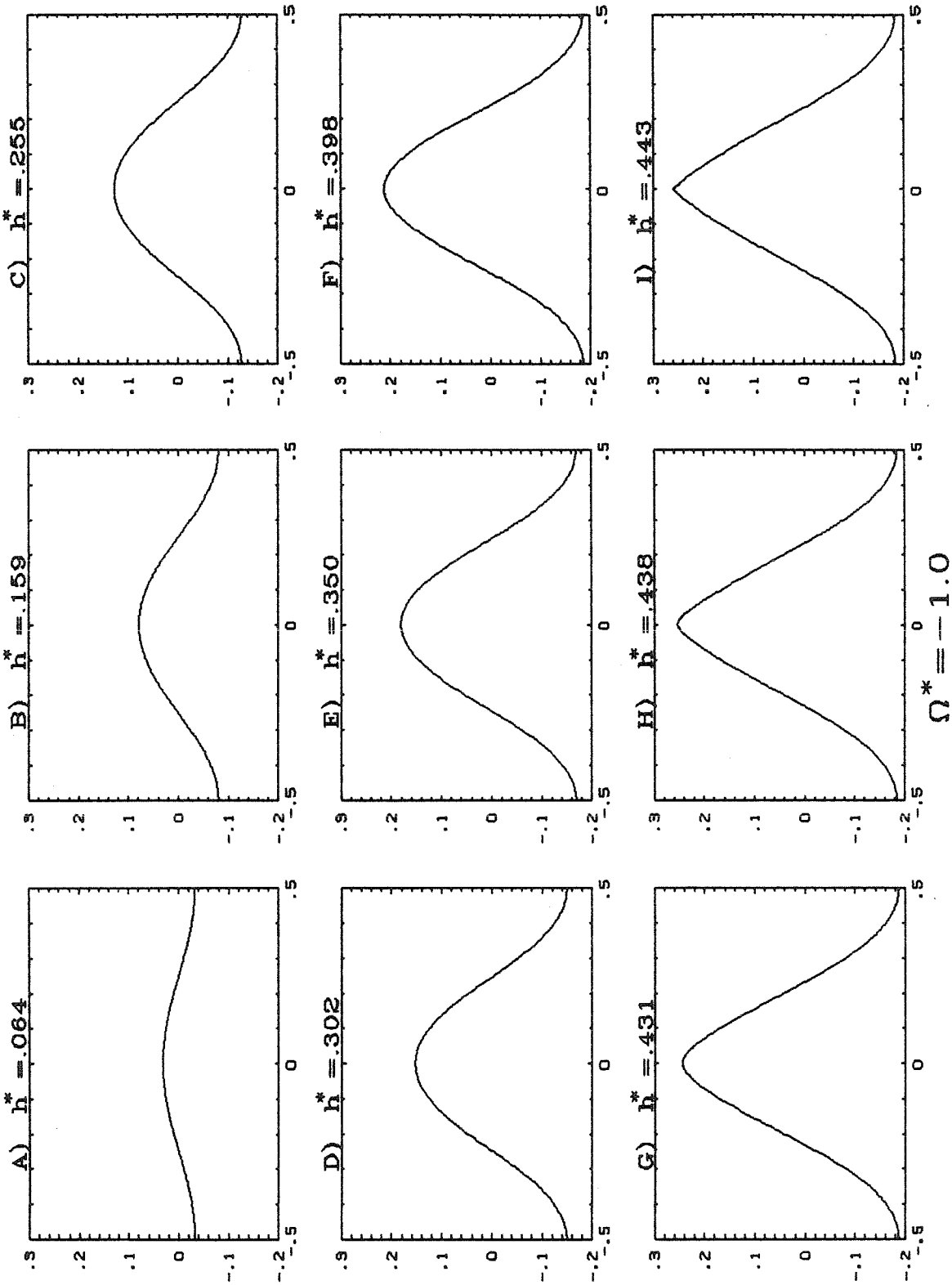


Figure 5-10

# EXTREME WAVE PROPERTIES
## (regular class 1 extreme waves)

| $\Omega^*$ | $h^*$ | $c^*$ | $T^*$ | $P^*$ | $I^*$ | crest angle |
|---|---|---|---|---|---|---|
| +1.5 | .03093 | .5454 | .00046 | .00106 | .00293 | 119° |
| +1.0 | .04931 | .6711 | .00175 | .00319 | .00774 | 119° |
| +0.5 | .08231 | .8453 | .00776 | .01035 | .02245 | 120° |
| 0.0 | .1411 | 1.093 | .03829 | .03457 | .07011 | 120° |
| −0.5 | .2452 | 1.478 | .2075 | .1166 | .2360 | 120° |
| −1.0 | .4431 | 2.268 | 1.423 | .4237 | .9437 | 120° |
| −1.5 | .9287 | 4.984 | 21.20 | 2.123 | 6.253 | 119° |

Figure 5-11

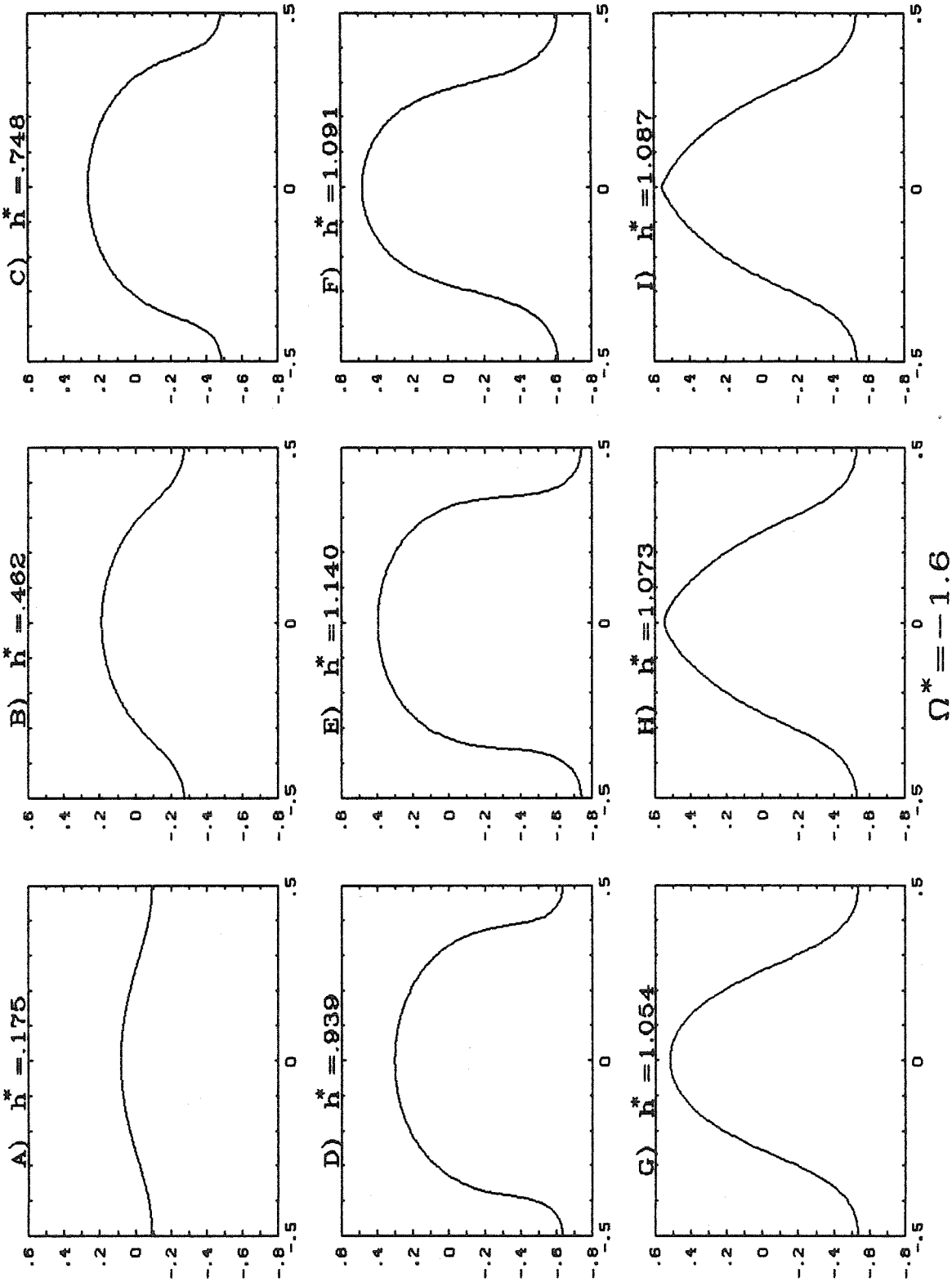
A) h* = .175
B) h* = .462
C) h* = .748
D) h* = .939
E) h* = 1.140
F) h* = 1.091
G) h* = 1.054
H) h* = 1.073
I) h* = 1.087
Ω* = −1.6

Figure 5-12

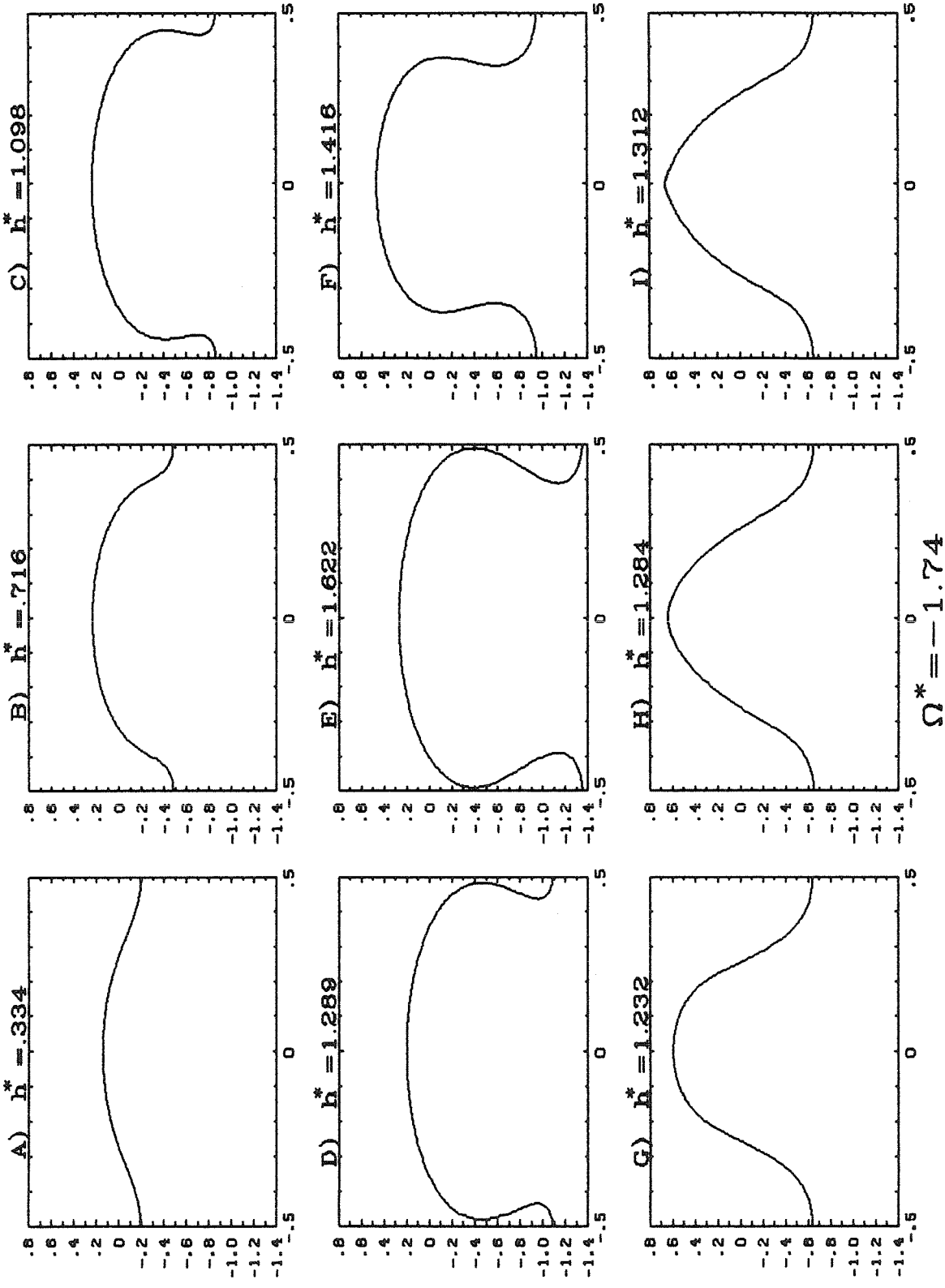
A) h* = .334
B) h* = .716
C) h* = 1.098
D) h* = 1.289
E) h* = 1.622
F) h* = 1.416
G) h* = 1.232
H) h* = 1.284
I) h* = 1.312
Ω* = −1.74

Figure 5-13

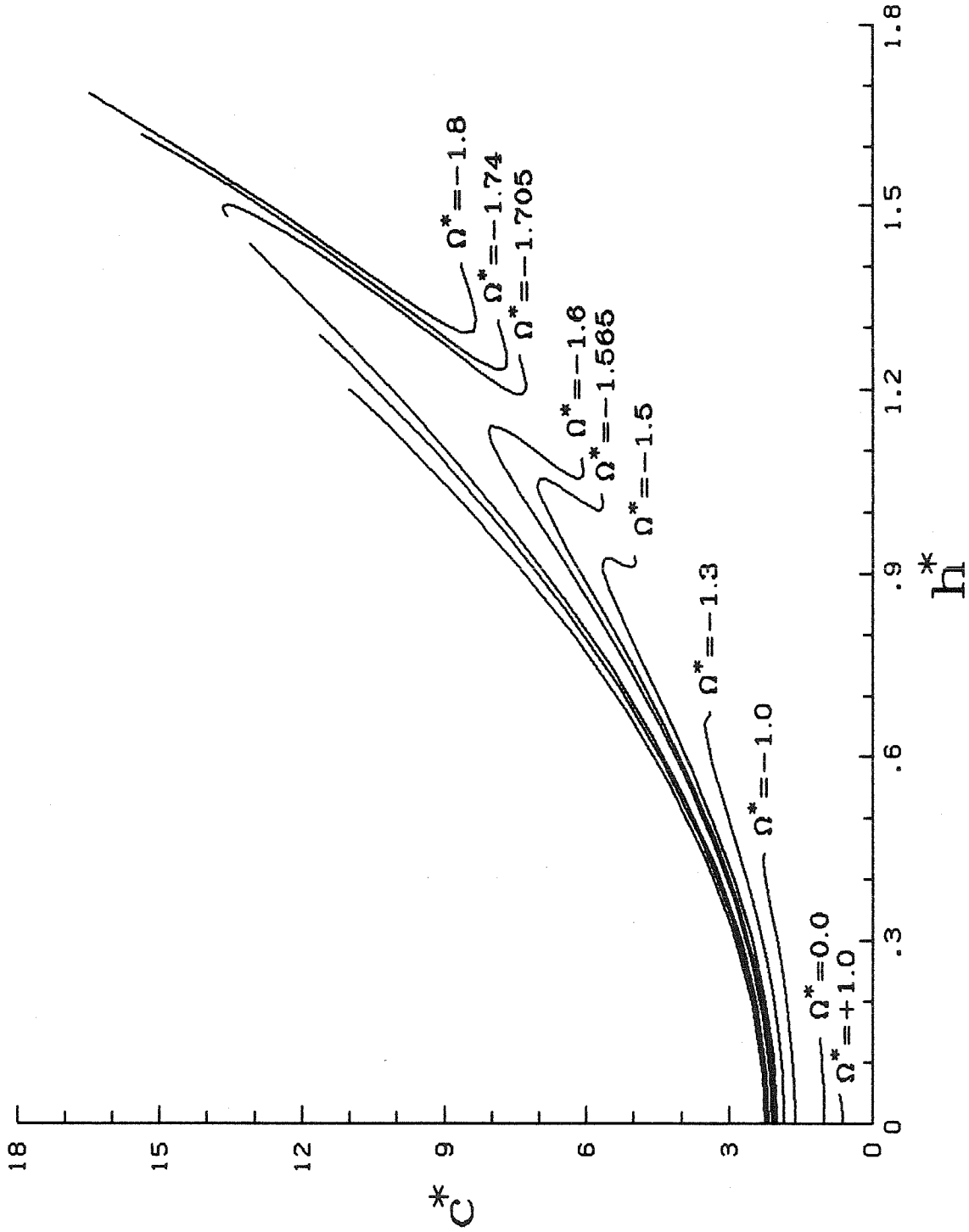
$\Omega^*=-1.8$
$\Omega^*=-1.74$
$\Omega^*=-1.705$
$\Omega^*=-1.6$
$\Omega^*=-1.565$
$\Omega^*=-1.5$
$\Omega^*=-1.3$
$\Omega^*=-1.0$
$\Omega^*=0.0$
$\Omega^*=+1.0$
$C^*$
$h^*$
0
3
6
9
12
15
18
.3
.6
.9
1.2
1.5
1.8

Figure 5-14

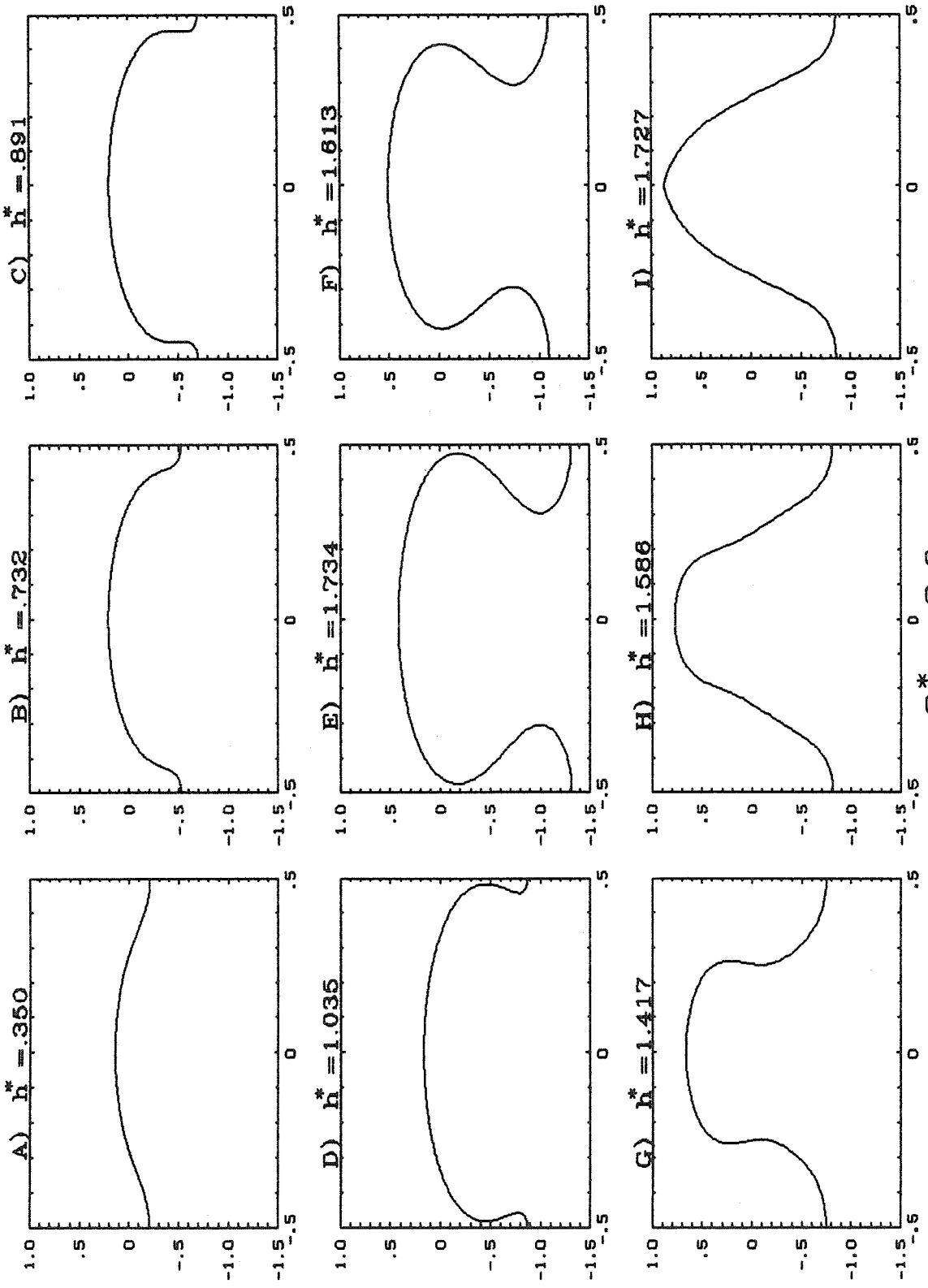
A) h* =.350
B) h* =.732
C) h* =.891
D) h* =1.035
E) h* =1.734
F) h* =1.813
G) h* =1.417
H) h* =1.586
I) h* =1.727
Ω* =−2.0

Figure 5-15

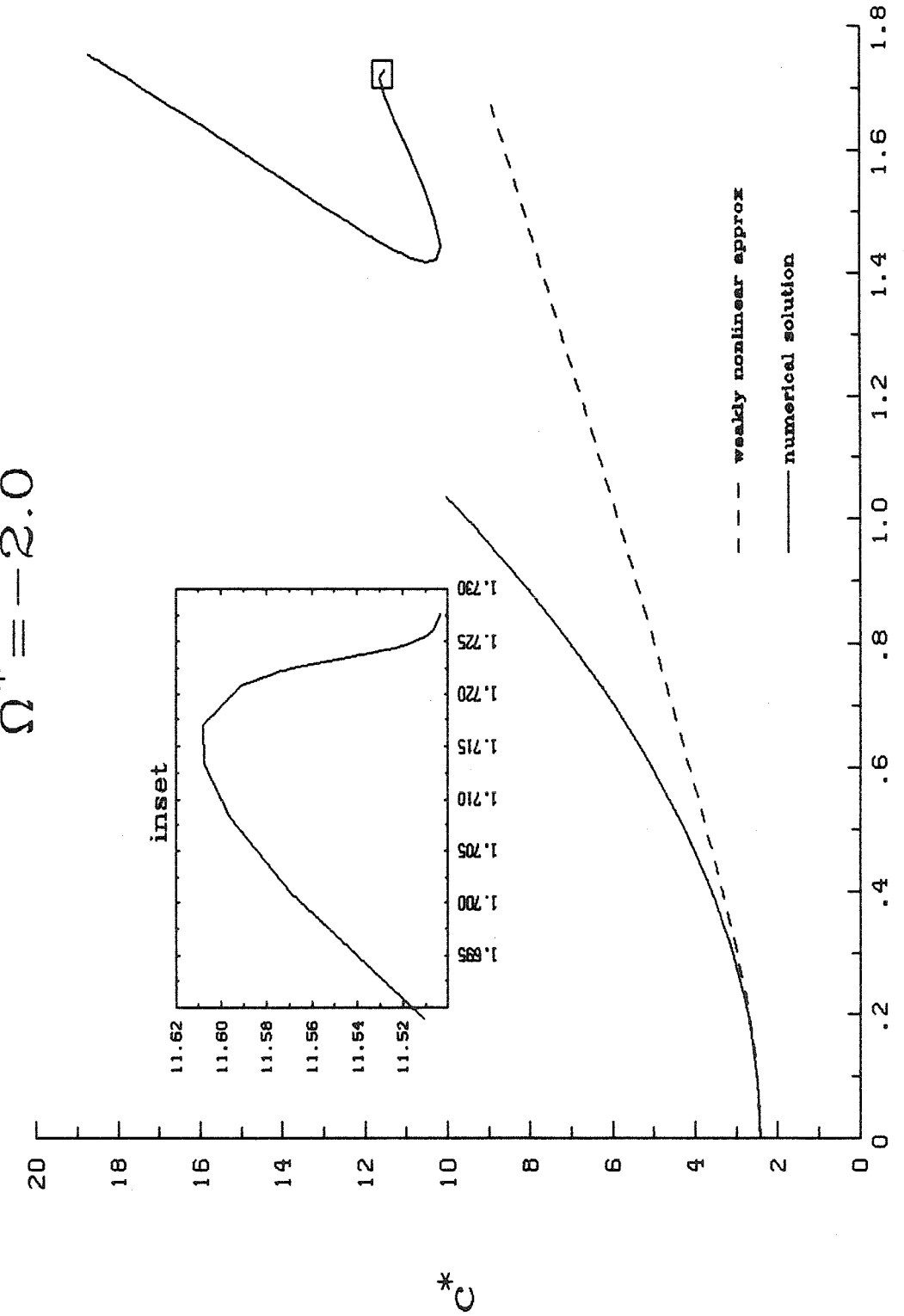
Ω*=−2.0
inset
11.62
11.60
11.58
11.56
11.54
11.52
1.730
1.725
1.720
1.715
1.710
1.705
1.700
1.695
20
18
16
14
12
10
8
6
4
2
0
.2
.4
.6
.8
1.0
1.2
1.4
1.6
1.8
h*
c*
weakly nonlinear approx
numerical solution

Figure 5-16

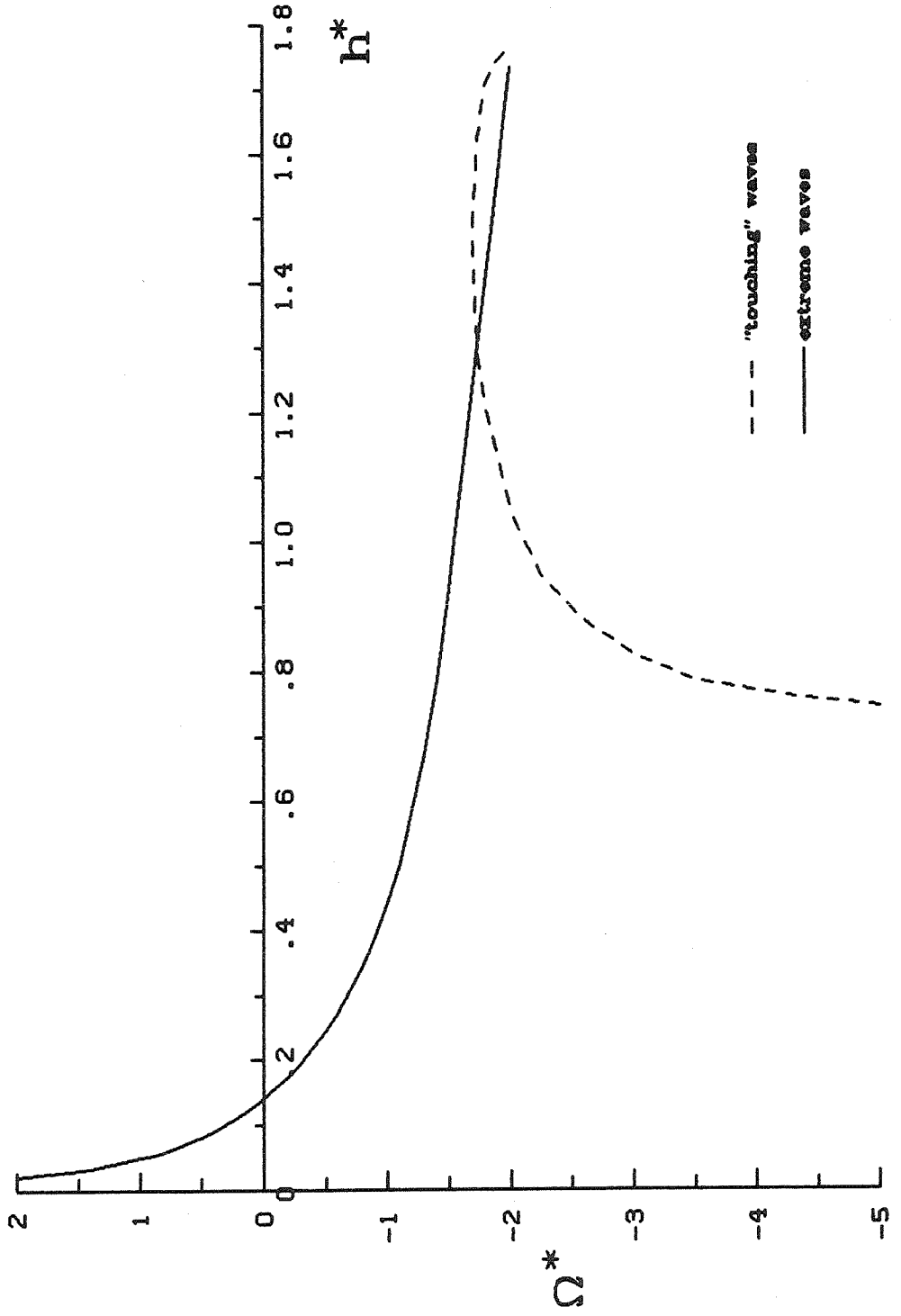
h*
Ω*
"touching" waves
extreme waves
2
1
0
-1
-2
-3
-4
-5
0
.2
.4
.6
.8
1.0
1.2
1.4
1.6
1.8

Figure 5-17

# SOME BIFURCATION POINT VALUES FOR REGULAR TO IRREGULAR WAVE TRANSITION

| | CLASS 2 | | CLASS 3 | |
|---|---|---|---|---|
| $\Omega^*$ | $h^*$ | $c^*$ | $h^*$ | $c^*$ |
| +1.0 | .03022 | .5387 | .02526 | .4703 |
| +.75 | .03640 | .5855 | .02690 | .5011 |
| +.50 | .04397 | .6383 | .03142 | .5383 |
| +.25 | .05322 | .6981 | .03672 | .5797 |
| 0.0 | .06446 | .7666 | .04294 | .6259 |
| −.25 | .07805 | .8460 | .05021 | .6780 |
| −.50 | .09447 | .9400 | .05868 | .7376 |
| −.75 | .1143 | 1.0544 | .06856 | .8069 |
| −1.0 | .1383 | 1.1988 | .08009 | .8894 |

Figure 5-18

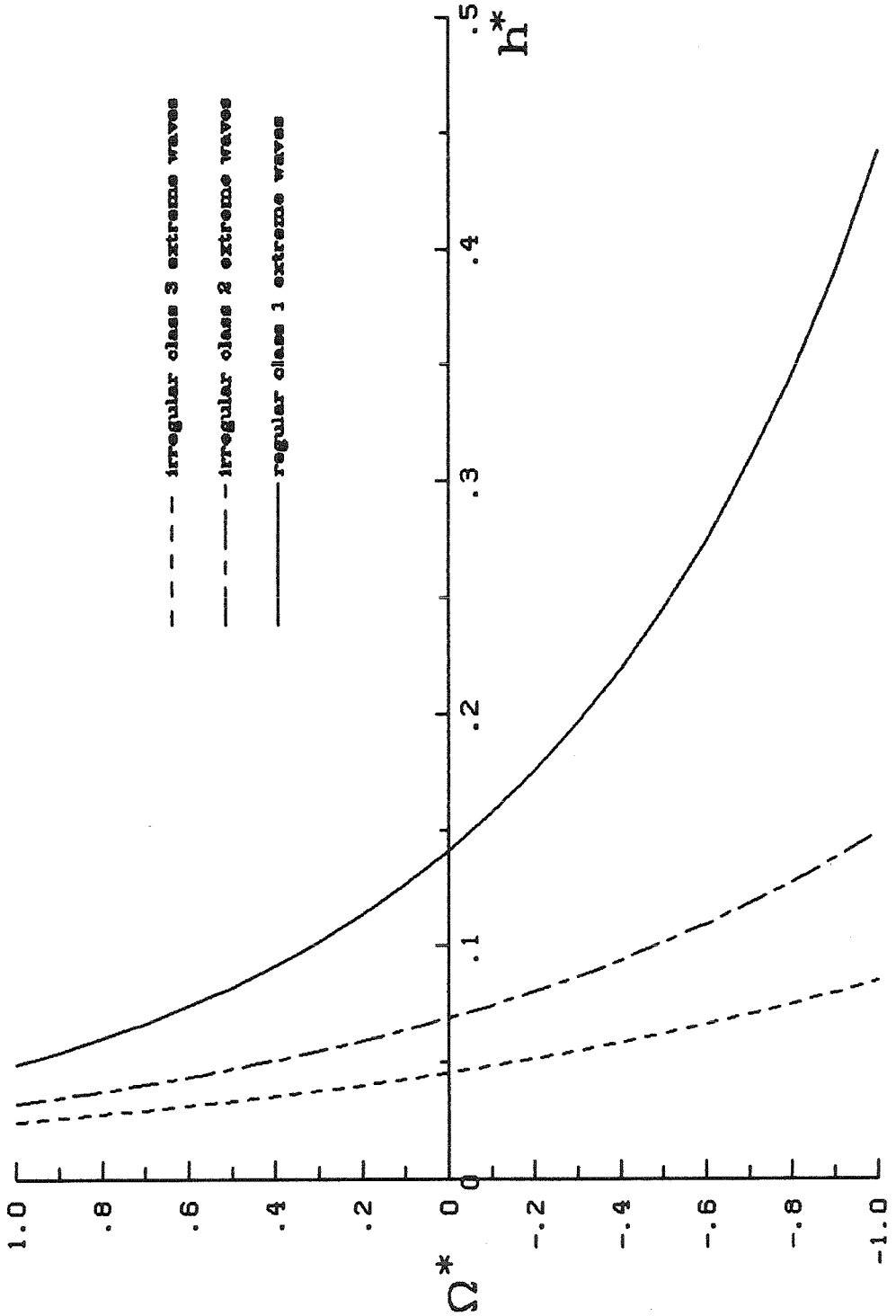
irregular class 3 extreme waves
irregular class 2 extreme waves
regular class 1 extreme waves
h*
Ω*
1.0
.8
.6
.4
.2
0
-.2
-.4
-.6
-.8
-1.0
.1
.2
.3
.4
.5

Figure 5-19

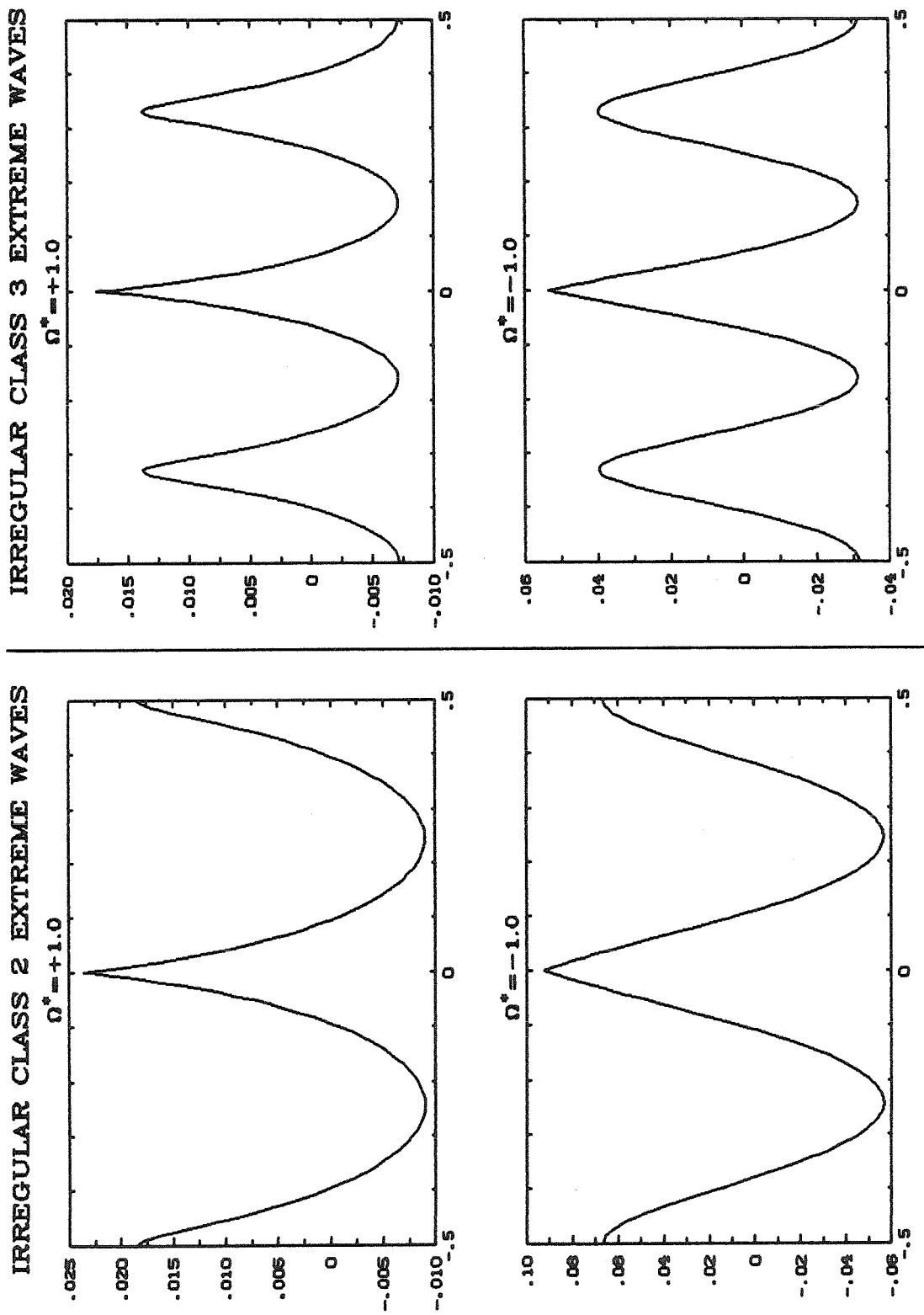
IRREGULAR CLASS 3 EXTREME WAVES
Ω*=+1.0
Ω*=-1.0
IRREGULAR CLASS 2 EXTREME WAVES
Ω*=+1.0
Ω*=-1.0

Figure 5-20

# CHAPTER 6

## A NOTE ON STABILITY

To examine the stability of finite-amplitude waves on a deep linear shear current a detailed numerical study is necessary. However, a simple argument indicates that the weakly nonlinear waves are unstable to modulational (long wavelength) disturbances. The argument proceeds as for the irrotational case. (See Whitham (1974)).

Since changes in the "mean velocity" and "mean height" play no role for deep water, pseudo frequencies and wave numbers do not arise. Therefore, modulations of the weakly nonlinear waves (found in chapter 2) will be described simply by

$$\frac{\partial a_1^2}{\partial t} + a_1^2\, \ddot{\omega}_0(k)\, \frac{\partial k}{\partial x'} + \dot{\omega}_0(k)\, \frac{\partial a_1^2}{\partial x'} = O(a_1^4) \tag{6.1}$$

$$\frac{\partial k}{\partial t} + \dot{\omega}_0(k)\, \frac{\partial k}{\partial x'} + \omega_2(k)\, \frac{\partial a_1^2}{\partial x'} = O(a_1^4) \quad . \tag{6.2}$$

Here $a_1^2$ and $k$ are slowly varying functions of $x'$ and $t$. The $\omega$'s are defined by $\omega_0(k) = c_0(k)\,k$ and $\omega_2(k) = c_2(k)\,k$ if the $c$'s are given by the dispersion relation $c(k) = c_0(k) + c_2(k)\,a_1^2 + O(a_1^4)$. The dot notation is used so that $\dot{\omega}_0(k) = \dfrac{d\omega_0}{dk}$, et cetera. For the general derivation of (6.1)-(6.2) from a variational principle see Whitham (1974).

If we neglect the $O(a_1^4)$ terms then the characteristics for the system (6.1)-(6.2) are given by

$$\frac{dx'}{dt} = \dot{\omega}_0(k) \pm [\omega_2(k)\,\ddot{\omega}_0(k)]^{\frac{1}{2}} a_1 \quad .$$

From the dispersion relation (2.2.7) it can be shown that

$$\omega_2 \ddot{\omega}_0 = \frac{-k^2(\dot{\omega}_0)^2}{\omega_0^2(2\omega_0+\Omega)^2}\,\sigma \quad ,$$

$$\text{where} \quad \sigma = \omega_0^4 - \tfrac{1}{2}\Omega^2\omega_0^2 + [\omega_0^2 + 2\Omega\omega_0 + \tfrac{1}{2}\Omega^2]^2 \quad .$$

Using the linear dispersion relation $\omega_0^2 + \Omega\omega_0 - gk = 0$ it is possible to deduce that $\sigma = \frac{1}{2}\Omega^2\omega_0^2 + 2gk\Omega^2 + \frac{1}{4}\Omega^4 + 2g^2k^2$ and hence $\sigma > 0$ for all real $\Omega$. This means that $\ddot{\omega}_0\,\omega_2 < 0$ which in turn implies that the characteristic velocities are imaginary and the system (6.1)-(6.2) is elliptic. As remarked in the irrotational case, periodic wavetrains are unstable when the modulation equations are elliptic.

## APPENDIX 1

### Part (a)

We shall prove that for periodic waves $w(z)$ is a periodic function; that is, if $\lambda$ is the wavelength so that $\Delta(z+\lambda) = \Delta(z)$, then $w(z+\lambda) = w(z)$. Obviously by

$$\Delta(z) = \frac{\partial \psi}{\partial y}(x,y) - i\,\frac{\partial \varphi}{\partial y}(x,y)$$

periodicity is equivalent to

$$\frac{\partial \varphi}{\partial y}(x+\lambda,y) = \frac{\partial \varphi}{\partial y}(x,y)$$
$$\frac{\partial \psi}{\partial y}(x+\lambda,y) = \frac{\partial \psi}{\partial y}(x,y) \quad .$$

Integration implies that

$$\varphi(x+\lambda,y) = \varphi(x,y) + g_1(x)$$
$$\psi(x+\lambda,y) = \psi(x,y) + g_2(x)$$

If now the condition that $\varphi$ , $\psi \to 0$ is applied in the limit as $y \to -\infty$, it becomes clear that $g_1 = g_2 \equiv 0$ and so $\varphi$ and $\psi$ are periodic (in $x$). Since $w(z) = \varphi + i\psi$, $w$ is also periodic.

### Part (b)

Here we show that for periodic waves, $|w(z)|$ is bounded for all $z$ in the fluid domain and its boundary. By (a) the range $0 \le x \le \lambda$ need only be considered. $\varphi$ , $\psi \to 0$ as $y \to -\infty$ uniformly in $x$ means that given $\varepsilon > 0$ there exists a $y_B$ such that $|\varphi| \le \varepsilon$ and $|\psi| \le \varepsilon$ whenever $y \le y_B$. Therefore in the region $R_1 = \{(x,y) \mid 0 \le x \le \lambda \text{ and } y \le y_B\}$, $|\varphi|$ and $|\psi|$ are bounded. Let $R_2$ be the region defined by $R_2 = \{(x,y) \mid 0 \le x \le \lambda \text{ and } y_B \le y \le H(x)\}$. $\varphi$ and $\psi$ are continuous in this closed and bounded region; hence, from a result in calculus the functions $|\varphi|$ and $|\psi|$ are bounded in $R_2$. Since $|w(z)| \le |\varphi| + |\psi|$ obviously $|w(z)|$ is bounded in $R_1 \cup R_2$.

## APPENDIX 2

In this appendix we verify that

$$\fint_{-mD}^{mD} \frac{f(\hat{\tau})}{\zeta(\tau)-\zeta(\hat{\tau})}\, d\hat{\tau} \;\rightarrow\; \frac{\pi}{\Lambda}\fint_{0}^{D} f(\hat{\tau})\, \cot\left(\frac{\pi}{\Lambda}[\zeta(\tau)-\zeta(\hat{\tau})]\right) d\hat{\tau} \quad \text{as} \quad m \rightarrow \infty \;. \tag{A2.1}$$

if $f(\tau+mD) = f(\tau)$. First observe that

$$\fint_{-mD}^{mD} \frac{f(\hat{\tau})}{\zeta(\tau)-\zeta(\hat{\tau})}\, d\hat{\tau} \;=\; \sum_{n=-m}^{m-1} \fint_{nD}^{(n+1)D} \frac{f(\hat{\tau})}{\zeta(\tau)-\zeta(\hat{\tau})}\, d\hat{\tau}$$

and then make the substitution $\hat{\tau} = \hat{t} + nD$ on the right hand side. Since $f(\hat{t}+nD) = f(\hat{t})$ and $\zeta(\hat{t}+nD) = \zeta(\hat{t}) + n\Lambda$ it can be shown that

$$\fint_{-mD}^{mD} \frac{f(\hat{\tau})}{\zeta(\tau)-\zeta(\hat{\tau})}\, d\hat{\tau} \;=\; \frac{1}{\Lambda}\fint_{0}^{D} f(\hat{\tau}) \left(\sum_{n=-m}^{m-1} \frac{1}{\left[\frac{\zeta(\tau)-\zeta(\hat{\tau})}{\Lambda}\right]-n}\right) d\hat{\tau} \;. \tag{A2.2}$$

Next consider the identity

$$\lim_{m\rightarrow\infty} \sum_{n=-m}^{m-1} \frac{1}{a-n} = \pi \cot \pi a \quad \text{if} \quad a \neq \text{integer} \;. \tag{A2.3}$$

If we let $a$ represent $\dfrac{\zeta(\tau)-\zeta(\hat{\tau})}{\Lambda}$, then using (A2.3) in (A2.2) as $m \rightarrow \infty$ gives the desired relation (A2.1).

# APPENDIX 3

We prove that

$$\frac{-i}{\Lambda}\int_0^D \cot\left(\frac{\pi}{\Lambda}[\zeta(\tau)-\zeta(\hat{\tau})]\right)\frac{d\zeta}{d\hat{\tau}}d\hat{\tau} = 1-\kappa(\tau) \quad . \tag{A3.1}$$

Application of the Cauchy Integral Formula and Plemelj's formula as in section 1.3 but now with $\Delta(z)$ replaced by the constant 1 leads to

$$1 = \frac{1}{2\pi i}\int_{-mD}^{mD}\frac{1}{\zeta(\tau)-\zeta(\hat{\tau})}\frac{d\zeta}{d\hat{\tau}}d\hat{\tau} + \frac{\kappa(\tau)}{2} + I_m(\zeta(\tau)) \quad , \tag{A3.2}$$

where

$$I_m(z) = \frac{1}{2\pi i}\int_{\Gamma_2(m)}\frac{1}{z-\hat{z}}d\hat{z} \quad .$$

$\Gamma_2(m)$ and $\kappa(\tau)$ are as before. In this case it is a simple observation that

$$\lim_{m\to\infty} I_m(z) = \frac{1}{2} \quad . \tag{A3.3}$$

Utilizing this fact and (A2.1) (from appendix 2) in the limit as $m \to \infty$ of (A3.2), we prove that relation (A3.1) holds.

APPENDIX 4

Here it is shown that

$$L\int_0^{2\pi} q^2(\tau)\,d\tau = c\Lambda \quad . \tag{A4.1}$$

Let the contour $\Gamma_0$ be defined by $\Gamma_0 = \{z \mid z = \zeta(\tau) \text{ and } 0 \le \tau < D\}$. Since $\Delta(z) = \frac{dw}{dz}$ and $w$ is periodic (by appendix 1a) it is clear that

$$\int_{\Gamma_0} \Delta(z)\,dz = w\Big|_{\Gamma_0} = 0 \quad . \tag{A4.2}$$

If we use the parametrization for $\Gamma_0$ and replace $\Delta(\zeta(\tau))$ by the right hand side of (1.3.10), then the real part of (A4.2) can be shown equivalent to

$$\int_0^D \left\{qN - [\Omega\beta - c]\frac{d\alpha}{d\tau}\right\} d\tau = 0 \quad . \tag{A4.3}$$

Here $N^2 = \frac{d\zeta}{d\tau}\frac{d\overline{\zeta}}{d\tau}$ has also been used. It follows that

$$\int_0^D qN\,d\tau = -\int_0^D c\,\frac{d\alpha}{d\tau}d\tau = -c\Lambda \tag{A4.4}$$

since by our choice of coordinates,

$$\int_0^D \beta(\tau)\frac{d\alpha}{d\tau}d\tau = 0 \quad .$$

Since $N = -L\,q$ and $D = 2\pi$ also by choice, (A4.1) follows from (A4.4).

REFERENCES

1. Amick, C.J., Fraenkel, L.E., and Toland, J.F. (1982). On the Stokes conjecture for the wave of extreme form. *Act. Math.* 148, 193-214.

2. Chen, B., and Saffman, P.G. (1980). Numerical evidence for the existence of new types of gravity waves on deep water. *Stud. Appl. Math.* 62, 1-21.

3. Dalrymple, R.A. (1974). A finite amplitude wave on a linear shear current. *J. Geophys.Res.* 79, 4498-4504.

4. Dalrymple, R.A., and Cox, J.C. (1976). Symmetric finite-amplitude rotational water waves. *J. Phys.Ocean.* 6, 847-852.

5. Dalrymple, R.A. (1977). A numerical model for periodic finite amplitude waves on a rotational fluid. *J. Computational Phys.* 24, 29-42.

6. Gerstner, F.J. (1802). *Abh. Bohm. Ges. Wiss.* 1(3), 1.

7. Keller, H.B. (1977). Numerical solution of bifurcation and nonlinear eigenvalue problems. *Applications of Bifurcation Theory.* 359-384. Academic Press, New York.

8. Longuet-Higgins, M.S. (1975). Integral properties of periodic gravity waves of finite amplitude. *Proc. Roy. Soc., Ser A.* 342, 157-174.

9. Longuet-Higgins, M.S., and Fox, M.J.H. (1978). Theory of the almost-highest wave. Part 2. Matching and analytic extension. *J. Fluid Mech.* 85, 769-786.

10. Luke, J.C. (1967). A variational principle for a fluid with a free surface. *J. Fluid Mech.* 27, 395-397.

11. McLean, J.W. (1982). Instabilities of finite amplitude water waves. *J. Fluid Mech.* 114, 315-330.

12. Miche, M. (1944). Mouvements ondulatories de la mer en profondeur constante ou decroissante. *Ann. Ponts Chaussees.* 114, 2-78, 131-164, 270-292, 386-406.

13. Michell, J.H. (1893). The highest waves in water. *Phil. Mag.* 36, 430-437.

14. Muskhelishvili, N.I. (1946). *Singular Integral Equations*. P. Noordhoff Ltd.

15. Rottman, J.W., and Olfe, D.B. (1980). Some new highest-wave solutions for deep-water waves of permanent form. *J. Fluid Mech.* 100, 801-810.

16. Stokes, G.G. (1847). On the theory of oscillatory waves. *Camb. Trans. Phil. Soc.* 8, 441-473.

17. Tsao, S. (1959). Behavior of surface waves on a linearly varying current. *Mosk. Fiz. Tekh. Inst. Issled. Mekh. Prikl. Mat.* 3, 66-84.

18. Whitham, G.B. (1967). Non-linear dispersion of water waves. *J. Fluid Mech.* 27, 399-412.

19. Whitham, G.B. (1974). *Linear and Nonlinear Waves*. John Wiley & Sons, New York.

20. Yamada, H. (1957). Highest waves of permanent type on the surface of deep water. *Rep. Res. Inst. Appl. Mech.* Kyushu Univ. 5, 37-52.